

SCREENING SARS-COV-2 MAIN PROTEASE INHIBITORY
ACTIVITY OF HERBAL EXTRACTS AND
DEVELOPMENT OF ALPHA-MANGOSTIN LOADED
POLYMERIC MICELLES



A Thesis Submitted in Partial Fulfillment of the Requirements
for the Degree of Master of Science in Pharmaceutical Sciences and
Technology
Faculty Of Pharmaceutical Sciences
Chulalongkorn University
Academic Year 2023

การคัดกรองฤทธิ์ยับยั้งเอนไซม์โปรตีเอสหลักของซาร์ส-โควี-2 ของสารสกัดสมุนไพร และการ
พัฒนาพอลิเมอร์ไมเซลล์บรรจุ แอลฟา-แมงโกสติน



วิทยานิพนธ์นี้เป็นส่วนหนึ่งของการศึกษาตามหลักสูตรปริญญาวิทยาศาสตรมหาบัณฑิต
สาขาวิชาเภสัชศาสตร์และเทคโนโลยี
คณะเภสัชศาสตร์ จุฬาลงกรณ์มหาวิทยาลัย
ปีการศึกษา 2566

Thesis Title SCREENING SARS-COV-2 MAIN
 PROTEASE INHIBITORY ACTIVITY OF
 HERBAL EXTRACTS AND DEVELOPMENT
 OF ALPHA-MANGOSTIN LOADED
 POLYMERIC MICELLES
By Miss Su Sundee Myint
Field of Study Pharmaceutical Sciences and Technology
Thesis Advisor Associate Professor SUPAKARN CHAMNI,
 Ph.D.
Thesis Co Advisor NATTIKA NIMMANO, Ph.D.

Accepted by the FACULTY OF PHARMACEUTICAL
SCIENCES, Chulalongkorn University in Partial Fulfillment of the
Requirement for the Master of Science

..... Dean of the FACULTY OF
 PHARMACEUTICAL
 SCIENCES
(Professor PORNANONG ARAMWIT, Ph.D.)

THESIS COMMITTEE

..... Chairman
(Assistant Professor CHAISAK
CHANSRINIYOM, Ph.D.)

..... Thesis Advisor
(Associate Professor SUPAKARN CHAMNI,
Ph.D.)

..... Thesis Co-Advisor
(NATTIKA NIMMANO, Ph.D.)

..... Examiner
(Associate Professor JITTIMA LUCKANAGUL,
Ph.D.)

..... External Examiner
(Assistant Professor Bodee Nutho, Ph.D.)

ชัชวาลย์ มินท์ : การคัดกรองฤทธิ์ยับยั้งเอนไซม์โปรตีนเอสหลักของซาร์ส-โควี-2 ของสารสกัดสมุนไพร และการพัฒนาพอลิเมอร์ไมเซลล์บรรจุอัลฟา-แมงโกสติน. (SCREENING SARS-COV-2 MAIN PROTEASE INHIBITORY ACTIVITY OF HERBAL EXTRACTS AND DEVELOPMENT OF ALPHA-MANGOSTIN LOADED POLYMERIC MICELLES) อ.ที่ปรึกษาหลัก : รศ. ดร.ศุภกาญจน์ ชำนิ, อ.ที่ปรึกษาร่วม : ดร.ณัฐธิดา นิมมะโน

โรคติดเชื้อไวรัสโคโรนาสายพันธุ์ใหม่ 2019 (โรคโควิด-19) จัดเป็นเป็นโรคติดเชื้อ การระบาดของโควิด-19 ที่เกิดขึ้นในเดือนธันวาคม 2562 ทำให้เกิดการระบาดครั้งใหญ่และส่งผลเสียต่อผู้คนทั่วโลก ทั้งการจืดจางและการรักษาที่มีความจำเป็นเพื่อให้การดูแลสุขภาพเพื่อต้านโควิด-19 อยู่ในระดับที่ควบคุมได้ มีการค้นพบและพัฒนาวัคซีนและยาใหม่ ๆ หลายชนิด แต่ปัญหาที่ยังไม่ได้รับการแก้ไขทั้งหมดเนื่องจากผลข้างเคียงจากยา เนื่องจากสมุนไพรแผนโบราณถูกนำมาใช้ในการรักษาโรคต่าง ๆ มาเป็นเวลหลายปี เพราะมีความปลอดภัยและประสิทธิภาพดี ดังนั้นการพัฒนาจากสารสกัดกัญชากัญชารวมชาติจึงอาจเป็นหนึ่งในวิธีการที่เป็นไปได้มากที่สุด สารออกฤทธิ์ทางชีวภาพบางชนิดจากสมุนไพรไทยได้รับการรายงานเมื่อไม่นานมานี้ว่ามีฤทธิ์ยับยั้งการทำงานของโปรตีนเอสหลักของซาร์สโควี-2 (3CL^{Pro}) ซึ่งเป็นเอนไซม์สำคัญในการแบ่งตัวของไวรัส ดังนั้นการศึกษานี้จึงมีวัตถุประสงค์เพื่อตรวจสอบศักยภาพของสารยับยั้ง 3CL^{Pro} จากสารสกัดสมุนไพร โดยการตรวจคัดกรองในหลอดทดลอง ผลการศึกษาพบว่าเหง้าขมิ้น รากชะเอมเทศ เมล็ดขี้หว่า และผลคิปปลี่มีฤทธิ์ยับยั้ง 3CL^{Pro} ได้ดี นอกจากนี้ยังพบว่าสารสกัดเปลือกของผลมังคุดมีฤทธิ์ยับยั้ง 3CL^{Pro} ในหลอดทดลองสูงสุด อัลฟา-แมงโกสตินซึ่งเป็นแซนโทนธรรมชาติที่ได้รับการศึกษามากที่สุดจากสารสกัดเปลือกมังคุดได้นำมาทำการศึกษาต่อการศึกษานี้เพื่อประเมินศักยภาพของฤทธิ์ยับยั้ง 3CL^{Pro} เพิ่มเติม เพื่อที่จะปรับปรุงความสามารถในการละลายและการดูดซึมอัลฟา-แมงโกสตินจึงถูกนำมาทำหุ้มด้วยไมเซลล์โพลีเมอร์ของ Soluplus® จากผลการศึกษาเบื้องต้น ไมเซลล์โพลีเมอร์ที่บรรจุอัลฟา-แมงโกสติน 5% โดยน้ำหนักที่เตรียมด้วย Soluplus® เข้มข้น 1 มก./มล. เป็นสูตรผสมที่เหมาะสมเนื่องจากประสิทธิภาพการห่อหุ้มและความสามารถในการบรรจุสูง จากนั้น Soluplus® และอัลฟา-แมงโกสตินที่ความเข้มข้นสูงขึ้นถูกนำมาใช้ในการศึกษาเพิ่มเติมเพื่อเพิ่มประสิทธิภาพการห่อหุ้ม ความสามารถในการบรรจุสารสำคัญ และคุณลักษณะอื่น ๆ ให้ดียิ่งขึ้น จากการศึกษาพบว่า สูตรผสม 5% w/w ซึ่งประกอบด้วย Soluplus® 10 มก./มล. และอัลฟา-แมงโกสติน 0.5 มก./มล. เป็นสูตรผสมที่เหมาะสมในแง่ของประสิทธิภาพการห่อหุ้มสูงสุดและความสามารถในการบรรจุสารสำคัญ นอกจากนี้ได้ทำการเปรียบเทียบลักษณะรูปร่างทรงกลมของไมเซลล์โพลีเมอร์ Soluplus® เปล่าและไมเซลล์โพลีเมอร์ Soluplus® ที่บรรจุอัลฟา-แมงโกสตินจากการวิเคราะห์ด้วย TEM สูตรผสมได้นำมาศึกษาความคงตัวโดยเก็บไว้ที่อุณหภูมิ 4°C ซึ่งพบว่ามีเสถียรภาพมากกว่าเมื่เก็บไว้ที่อุณหภูมิห้อง แม้ว่าเปอร์เซ็นต์ (%) การยับยั้งของไมเซลล์โพลีเมอร์ที่บรรจุอัลฟา-แมงโกสตินต่อ 3CL^{Pro} จะต่ำกว่าการยับยั้งของอัลฟา-แมงโกสตินที่ไม่ได้บรรจุในระบับนำส่งแบบนาโนแต่ผลการยับยั้ง 3CL^{Pro} ยังอยู่ในระดับที่น่าพอใจ เพราะยับยั้งได้มากกว่า 50% อย่างไรก็ตามอัลฟา-แมงโกสตินที่บรรจุในไมเซลล์โพลีเมอร์แสดง % การมีชีวิตของเซลล์ที่สูงกว่าอัลฟา-แมงโกสตินที่ไม่ได้บรรจุในระบับนำส่งแบบนาโน โดยสรุป อัลฟา-แมงโกสตินสามารถบรรจุในไมเซลล์โพลีเมอร์ Soluplus® ได้อย่างมีประสิทธิภาพสูงและแสดงฤทธิ์ยับยั้ง 3CL^{Pro} ของของซาร์สโควี-2 ได้พร้อมกับแสดงความเป็นพิษต่อเซลล์ต่ำซึ่งจะเป็นประโยชน์สำหรับการศึกษาต่อไป

จุฬาลงกรณ์มหาวิทยาลัย
CHULALONGKORN UNIVERSITY

สาขาวิชา
ปีการศึกษา

เภสัชศาสตร์และเทคโนโลยี
2566

ลายมือชื่อนิติ
ลายมือชื่อ อ.ที่ปรึกษาหลัก
ลายมือชื่อ อ.ที่ปรึกษาร่วม

6472002933 : MAJOR PHARMACEUTICAL SCIENCES AND TECHNOLOGY

KEYWORD: 3CL^{Pro} INHIBITORY ACTIVITY/ ALPHA-MANGOSTIN/ SOLUPLUS®/ POLYMERIC MICELLES

Su Sundee Myint : SCREENING SARS-COV-2 MAIN PROTEASE INHIBITORY ACTIVITY OF HERBAL EXTRACTS AND DEVELOPMENT OF ALPHA-MANGOSTIN LOADED POLYMERIC MICELLES. Advisor: Assoc. Prof. SUPAKARN CHAMNI, Ph.D. Co-advisor: NATTIKA NIMMANO, Ph.D.

The coronavirus disease 19 (COVID-19) is an infectious disease. The outbreak of COVID-19 that emerged in December 2019 has caused a serious pandemic and detrimental impacts on people worldwide. Both vaccinations and treatments are needed to achieve the comprehensive level of health care against COVID-19. Several novel vaccines and drugs have been discovered and developed, but the problem has not been fully resolved due to their associated adverse effects. Since traditional herbal medicines have been used for many years in various disease treatments due to their safety and efficacy, developing natural product-based drugs could be one of the most promising strategies. Some of the bioactive compounds from Thai herbs have been reported recently for their potential inhibitory activity towards SARS-CoV-2 main protease (3CL^{Pro}), which is a key enzyme for viral replication. Hence, this study aims to investigate the potential 3CL^{Pro} inhibitor from herbal extracts by an *in vitro* screening. The results showed that turmeric rhizome, licorice root, sweet fennel seeds and long pepper fruits had promising 3CL^{Pro} inhibitory activity. It was also investigated that the pericarp extract of mangosteen fruit had the highest *in vitro* 3CL^{Pro} inhibitory activity. Alpha-mangostin which is the most studied natural xanthone from mangosteen pericarp extract has been selected as the interested bioactive compound in this study to further evaluate its potential SARS-CoV-2 main protease inhibitory activity. In order to improve the solubility and bioavailability, alpha-mangostin was encapsulated in Soluplus® polymeric micelles. Based on the preliminary results, 5% w/w alpha-mangostin loaded polymeric micelles prepared with Soluplus® concentration of 1 mg/mL seemed to be the promising formulation due to its high encapsulation efficiency and loading capacity. Then, higher Soluplus® concentrations and higher alpha-mangostin concentrations were used to investigate further for higher encapsulation efficiency, loading capacity and the other characterization parameters. It was investigated that the 5%w/w formulation which was made up of 10 mg/mL Soluplus® and 0.5 mg/mL alpha-mangostin, was the promising formulation in terms of the highest encapsulation efficiency and loading capacity as well as the desirable characterizations results. The spherical shape of both blank Soluplus® polymeric micelles and alpha-mangostin loaded Soluplus® polymeric micelles was noted from TEM analysis. Regarding the stability, the formulation kept at 4°C seemed to be more stable as compared to the one kept at room temperature. Although the percent (%) inhibition of alpha-mangostin loaded polymeric micelles towards 3CL^{Pro} was lower than that of alpha-mangostin compound without the nanocarrier, it could still be considered as the promising formulation because its % inhibition towards 3CL^{Pro} was more than 50%. Moreover, alpha-mangostin loaded in polymeric micelles displayed higher %cell viability than alpha-mangostin compound without the nanocarrier. Overall, alpha-mangostin can be loaded in Soluplus® polymeric micelles with high efficiency, and it showed the promising results towards SARS-CoV-2 main protease (3CL^{Pro}) inhibitory activity with lower cytotoxicity which will be useful for further studies.

CHULALONGKORN UNIVERSITY

Field of Study: Pharmaceutical Sciences and
Technology

Academic Year: 2023

Student's Signature

Advisor's Signature

Co-advisor's Signature

ACKNOWLEDGEMENTS

First of all, I would like to express my sincere thanks to my advisor, Associate Professor Dr. Supakarn Chamni from Department of Pharmacognosy and Pharmaceutical Botany, Faculty of Pharmaceutical Sciences, Chulalongkorn University, for her advice, guidance and support throughout the process of this thesis and my research work.

I would also like to extend my gratitude to my co-advisor, Dr. Nattika Nimmano from Department of Pharmaceutics and Industrial Pharmacy, Faculty of Pharmaceutical Sciences, Chulalongkorn University, for her advice, guidance and support for my research work and thesis.

Moreover, I would like to show my appreciation to the thesis committee members for their comments and suggestions towards my thesis.

Furthermore, I am thankful to Miss Patcharin Wilasluck from Department of Biochemistry, Faculty of Science, Chulalongkorn University, for her help in the in vitro screening process of herbal extracts for SARS-CoV-2 main protease inhibitory activity. And also, I am thankful to Miss Aye Chan Khine Lin from Department of Pharmacognosy and Pharmaceutical Botany, Faculty of Pharmaceutical Sciences, Chulalongkorn University, for her help in the in vitro cytotoxicity study in HaCaT cells line.

Last but not least, I would like to thank Office of Academic Affairs, Chulalongkorn University for providing the Graduate Program Scholarship for ASEAN and NON-ASEAN Countries.

Finally, I would like to express my deepest gratitude towards my family for their love, encouragement and support throughout my life.

Su Sundee Myint

TABLE OF CONTENTS

	Page
.....	iii
ABSTRACT (THAI)	iii
.....	iv
ABSTRACT (ENGLISH).....	iv
ACKNOWLEDGEMENTS.....	v
TABLE OF CONTENTS.....	vi
LIST OF TABLES.....	x
LIST OF FIGURES.....	xi
CHAPTER 1. INTRODUCTION.....	1
1.1. Research Problem, Rationale and Significance.....	1
1.2. Research Objectives.....	3
1.3. Novelty of Research.....	4
1.4. Research Hypothesis.....	4
CHAPTER 2. LITERATURE REVIEW.....	5
2.1. Potential SARS-CoV-2 main protease (3CL ^{Pro}) inhibitory activity from herbal extracts.....	5
2.2. Pharmacological activities and potential SARS-CoV-2 main protease (3CL ^{Pro}) inhibitory activity of alpha-mangostin.....	7
2.3. Soluplus [®] polymeric micelles as the promising nanocarrier for hydrophobic compounds.....	9
2.3.1. Significance of Soluplus [®] in development of polymeric micelles.....	11
CHAPTER 3. RESEARCH METHODOLOGY.....	15
3.1. Herbal materials.....	15
3.2. Chemicals and reagents.....	16
3.3. Preparation of herbal extracts.....	16

3.4. Screening of mangosteen pericarp extract along with selected Thai herbal extracts for SARS-CoV-2 main protease (3CL ^{Pro}) inhibitory activity	17
3.5. Preparation of alpha-mangostin loaded polymeric micelles.....	18
3.5.1. Preparation of 2.5% w/w alpha-mangostin loaded polymeric micelles with Soluplus [®] concentration of 1 mg/mL.....	19
3.5.2. Preparation of 5% w/w alpha-mangostin loaded polymeric micelles with Soluplus [®] concentration of 1 mg/mL	20
3.5.3. Preparation of 10% w/w alpha-mangostin loaded polymeric micelles with Soluplus [®] concentration of 1 mg/mL.....	21
3.5.4. Preparation of 5% w/w alpha-mangostin loaded polymeric micelles with Soluplus [®] concentration of 2 mg/mL	22
3.5.5. Preparation of 5% w/w alpha-mangostin loaded polymeric micelles with Soluplus [®] concentration of 4 mg/mL	23
3.5.6. Preparation of 5% w/w alpha-mangostin loaded polymeric micelles with Soluplus [®] concentration of 10 mg/mL.....	24
3.6. Determination of encapsulation efficiency and loading capacity.....	25
3.6.1. Separation of non-incorporated/non-encapsulated alpha-mangostin	25
3.6.2. Evaluation of % encapsulation efficiency and % loading capacity by UV	26
3.6.3. Evaluation % encapsulation efficiency and % loading capacity by HPLC	27
3.7. Characterization of alpha-mangostin loaded polymeric micelles.....	28
3.8. Stability study of alpha-mangostin loaded polymeric micelles.....	29
3.9. Evaluation of SARS-CoV-2 main protease (3CL ^{Pro}) inhibitory activity of alpha-mangostin in polymeric micelles.....	29
3.10. Evaluation of <i>in vitro</i> cytotoxicity of alpha-mangostin in polymeric micelles in HaCaT cells line	29
3.11. Data analysis.....	31
CHAPTER 4. RESULTS AND DISCUSSION.....	32
4.1. Screening of mangosteen pericarp extract along with 27 herbal extracts for SARS-CoV-2 main protease (3CL ^{Pro}) inhibitory activity	32
4.1.1. Discussion	35

4.2. Preparation of alpha-mangostin loaded polymeric micelles with Soluplus [®] concentration of 1 mg/mL	36
4.2.1. Preliminary analyses of encapsulation efficiency (%EE) and loading capacity (%LC) of alpha-mangostin loaded polymeric micelles with UV-vis spectrophotometer.....	36
4.2.2. Preliminary analyses of encapsulation efficiency (%EE) and loading capacity (%LC) of alpha-mangostin loaded polymeric micelles with HPLC.....	38
4.2.3. Preliminary characterizations of alpha-mangostin loaded polymeric micelles.....	40
4.2.4. Discussion	41
4.3. Preparation of 5% w/w alpha-mangostin loaded polymeric micelles with Soluplus [®] concentration of 2 mg/mL	42
4.3.1. HPLC analyses of encapsulation efficiency (%EE) and loading capacity (%LC) of 5% w/w alpha-mangostin loaded polymeric micelles with Soluplus [®] concentration of 2 mg/mL	42
4.3.2. Characterizations of 5% w/w alpha-mangostin loaded polymeric micelles with Soluplus [®] concentration of 2 mg/mL	43
4.4. Preparation of 5% w/w alpha-mangostin loaded polymeric micelles with Soluplus [®] concentration of 4 mg/mL	44
4.4.1. HPLC analyses of encapsulation efficiency (%EE) and loading capacity (%LC) of 5% w/w alpha-mangostin loaded polymeric micelles with Soluplus [®] concentration of 4 mg/mL	44
4.4.2. Characterizations of 5% w/w alpha-mangostin loaded polymeric micelles with Soluplus [®] concentration of 4 mg/mL	45
4.5. Preparation of 5% w/w alpha-mangostin loaded polymeric micelles with Soluplus [®] concentration of 10 mg/mL	45
4.5.1. HPLC analyses of encapsulation efficiency (%EE) and loading capacity (%LC) of 5% w/w alpha-mangostin loaded polymeric micelles with Soluplus [®] concentration of 10 mg/mL	46
4.5.2. Characterizations of 5% w/w alpha-mangostin loaded polymeric micelles with Soluplus [®] concentration of 10 mg/mL	46
4.6. Discussion.....	47

4.7. Morphology analysis of 5%w/w alpha-mangostin loaded polymeric micelles with 10 mg/mL Soluplus [®] and 0.5 mg/mL alpha-mangostin	50
4.7.1. Discussion	52
4.8. Stability study of 5%w/w alpha-mangostin loaded polymeric micelles with 10 mg/mL Soluplus [®] and 0.5 mg/mL alpha-mangostin	53
4.8.1. Discussion	54
4.9. Comparative evaluations of SARS-CoV-2 main protease (3CL ^{Pro}) inhibitory activity of alpha-mangostin without the nanocarrier and alpha-mangostin loaded in polymeric micelles	56
4.9.1. Discussion	57
4.10. Comparative <i>in vitro</i> cytotoxicity evaluations of alpha-mangostin without nanocarrier and alpha-mangostin loaded in polymeric micelles	58
4.10.1. Discussion	59
CHAPTER 5. CONCLUSIONS	60
REFERENCES	63
APPENDICES	67
Appendix 1. Copyright guideline of CC-BY license version 4.0	67
Appendix 2. Copyright guideline of Frontiers Journal under CC-BY 4.0 License	69
Appendix 3. Copyright guideline of Journal of Complementary and Traditional Medicine under CC-BY 4.0 License	70
Appendix 4. Copyright guideline of Molecules (MDPI) Journal under CC-BY 4.0 License	71
VITA	72

LIST OF TABLES

	Page
Table 1. List of selected herbal materials used for in vitro screening of 3CL ^{Pro}	15
Table 2. <i>In vitro</i> SARS-CoV-2 main protease (3CL ^{Pro}) inhibition of herbal extracts at 0.1 mg/mL.....	33
Table 3. Analysis of alpha-mangostin content with UV-vis spectrophotometer	37
Table 4. Preliminary analyses of %EE and %LC with UV-vis spectrophotometer....	38
Table 5. Analysis of alpha-mangostin content with HPLC	39
Table 6. Preliminary HPLC analyses of %EE and %LC of 5% w/w alpha-mangostin loaded polymeric micelles formulation at Soluplus [®] concentration of 1 mg/mL.....	40
Table 7. Preliminary characterizations of alpha-mangostin loaded polymeric micelles	40
Table 8. HPLC analyses of %EE and %LC of 5% w/w alpha-mangostin loaded polymeric micelles formulation at Soluplus [®] concentration of 2 mg/mL	43
Table 9. Characterizations of 5% w/w alpha-mangostin loaded polymeric micelles with Soluplus [®] concentration of 2 mg/mL.....	43
Table 10. HPLC analyses of %EE and %LC of 5% w/w alpha-mangostin loaded polymeric micelles formulation at Soluplus [®] concentration of 4 mg/mL	44
Table 11. Characterizations of 5% w/w alpha-mangostin loaded polymeric micelles with Soluplus [®] concentration of 4 mg/mL.....	45
Table 12. HPLC analyses of %EE and %LC of 5% w/w alpha-mangostin loaded polymeric micelles formulation at Soluplus [®] concentration of 10 mg/mL	46
Table 13. Characterizations of 5% w/w alpha-mangostin loaded polymeric micelles with Soluplus [®] concentration of 10 mg/mL.....	47
Table 14. Summary of % EE, %LC and Characterizations of 5% w/w formulations .	48
Table 15. Characterizations of blank Soluplus [®] polymeric micelles and alpha-mangostin loaded Soluplus [®] polymeric micelles	53
Table 16. Stability study of 5% w/w alpha-mangostin loaded polymeric micelles.....	54

LIST OF FIGURES

	Page
Figure 1. Structure of SARS-CoV-2 main protease (3CL ^{Pro}) with substrate binding pocket.....	5
Figure 2. The binding pattern of rutin with conserved substrate-binding pocket of 3CL ^{Pro}	7
Figure 3. Chemical structure of alpha-mangostin.....	7
Figure 4. Interaction profile of alpha-mangostin (red structure) at the binding pocket of main protease active site.....	9
Figure 5. Chemical Structure of Soluplus [®]	10
Figure 6. Self-assembly process of Soluplus [®] micelles.....	11
Figure 7. Preparation of herbal extracts	17
Figure 8. Screening of mangosteen pericarp extract along with selected Thai herbal extracts for SARS-CoV-2 main protease (3CL ^{Pro}) inhibitory activity.....	18
Figure 9. Alpha-mangostin loaded Soluplus [®] polymeric micelles	19
Figure 10. Preparation of 2.5% w/w alpha-mangostin loaded polymeric micelles with Soluplus [®] concentration of 1 mg/mL.....	20
Figure 11. Preparation of 5% w/w alpha-mangostin loaded polymeric micelles with Soluplus [®] concentration of 1 mg/mL.....	21
Figure 12. Preparation of 10% w/w alpha-mangostin loaded polymeric micelles with Soluplus [®] concentration of 1 mg/mL.....	22
Figure 13. Preparation of 5% w/w alpha-mangostin loaded polymeric micelles with Soluplus [®] concentration of 2 mg/mL.....	23
Figure 14. Preparation of 5% w/w alpha-mangostin loaded polymeric micelles with Soluplus [®] concentration of 4 mg/mL.....	24
Figure 15. Preparation of 5% w/w alpha-mangostin loaded polymeric micelles with Soluplus [®] concentration of 10 mg/mL.....	25
Figure 16. Evaluations of SARS-CoV-2 main protease (3CL ^{Pro}) inhibitory activity and <i>in vitro</i> cytotoxicity of alpha-mangostin without nanocarrier and alpha-mangostin loaded in polymeric micelles	30

Figure 17. SARS-CoV-2 main protease (3CL ^{Pro}) inhibition of herbal extracts (H01-H27 and mangosteen pericarp)	34
Figure 18. 3CL ^{Pro} inhibitory activities of the most active herbal crude extracts at 0.1 mg/mL.....	34
Figure 19. Standard calibration curve for quantification of alpha-mangostin with UV	37
Figure 20. Standard calibration curve for quantification of alpha-mangostin with HPLC	39
Figure 21. TEM image of blank Soluplus [®] polymeric micelles	51
Figure 22. TEM image of 5% w/w alpha-mangostin loaded Soluplus [®] polymeric micelles	51
Figure 23. Physical appearances of blank Soluplus [®] polymeric micelles and alpha-mangostin loaded Soluplus [®] polymeric micelles	52
Figure 24. SARS-CoV-2 main protease (3CL ^{Pro}) activity of samples.....	56
Figure 25. 3CL ^{Pro} inhibitory activities of control and samples	57
Figure 26. %Cell viability evaluation of alpha-mangostin dissolved in DMSO (AM001) and alpha-mangostin loaded in polymeric micelles (AM008) against HaCaT cells line	58

CHAPTER 1. INTRODUCTION

1.1. Research Problem, Rationale and Significance

The coronavirus disease 19 (COVID-19) is an infectious disease that emerged in December 2019 from the predominantly airborne transmitted severe acute respiratory syndrome coronavirus 2 (SARS-CoV-2) (1). The outbreak of COVID-19 is a serious worldwide pandemic that has caused detrimental impacts on the lives of people with critical illnesses and millions of global death tolls (2). This has raised the attention of researchers to discover and develop novel vaccines and drugs for the comprehensive level of health care against COVID-19. Although there are treatments currently available, the problem has not been fully resolved due to their associated adverse effects. Therefore, the development of natural-product based drugs is one of the most promising approaches. This is because medicinal properties have been identified from the plant extracts, and traditional herbal medicines have been used for many years as safe and effective treatments in various diseases, including viral infections (3). Main protease (M^{Pro}), which is also known as 3-chymotrypsin-like protease ($3CL^{Pro}$) is a key enzyme involved in replication and transcription of SARS-CoV-2 virus (4). Recent studies have reported that some of the bioactive compounds from Thai herbs show potential SARS-CoV-2 main protease inhibitory activity (5-9). Hence, screening of herbal extracts and investigation of bioactive compounds that can target the inhibition of SARS-CoV-2 main protease is an essential strategy for discovery and development of the potential treatment against COVID-19.

Mangosteen (*Garcinia mangostana* Linn.) is a tropical plant that belongs to the Clusiaceae family. It is commonly found in Thailand as well as other Southeast Asian countries, and the fruit is well known as ‘queen of the fruits’. Besides its delightful

taste, the mangosteen fruit has numerous medicinal benefits (10, 11). The fruit rind or pericarp of mangosteen contains various phytochemicals such as- xanthenes, flavonoids, anthocyanins, tannins, isoflavones and phenolic acids. But, the major chemical constituents present in the pericarp extract are xanthenes. They are polyphenolic secondary metabolites, and the examples of xanthenes are- alpha-mangostin, beta-mangostin, gamma-mangostin, gartanin and 8-deoxygartanin (10, 11). Among all the natural xanthenes from *G. mangostana*, alpha-mangostin is mostly studied due to its highest percentage yield from the dry mangosteen pericarp extract, and its wide range of pharmacological properties (11). The anti-oxidant, anti-cancer, anti-inflammatory, anti-bacterial and anti-viral activities of alpha-mangostin have been reported in several studies (12-16). In addition, the potential SARS-CoV-2 main protease inhibitory activity of alpha-mangostin has been investigated recently (8, 17, 18). However, the hydrophobic nature of alpha-mangostin limits its biological activities and therapeutic efficacy (19). To overcome this limitation, alpha-mangostin loaded nanocarriers have been designed. Despite the availability of different nanocarriers, polymeric micelles could be the promising nanocarrier for hydrophobic bioactive compounds due to the presence of a robust core-shell structure of polymeric micelles and their intrinsic ability to improve the solubility of hydrophobic compounds, thereby enhancing their bioavailability and pharmacological activities.

Soluplus[®] is an amphiphilic polyvinyl caprolactam-polyvinyl acetate-polyethylene glycol graft copolymer. The grafting ratio is 57% polyvinyl caprolactam, 30% polyvinyl acetate and 13% polyethylene glycol by molecular weight (20, 21). However, the exact degree of grafting has not been reported. The molecular weight of

Soluplus can vary between 90,000 g/mol and 140,000 g/mol, but its average weight has been reported as 118,000 g/mol (20, 21). Soluplus consists of polyethylene glycol (PEG) as its hydrophilic backbone, and polyvinyl caprolactam with polyvinyl acetate side chains as its hydrophobic core (21). Soluplus[®] has a low critical micelle concentration (CMC) of 7.6 µg/mL (7.6 mg/L) which can facilitate to form self-assembled micelles in aqueous solution that is above its CMC (22-24). Due to its biocompatibility, biodegradability and excellent solubilizing property, Soluplus[®] has been widely used in nanotechnology-based drug delivery systems for hydrophobic drugs and bioactive compounds (22-25). In this research, Soluplus[®] polymeric micelles is used as the nanocarrier to encapsulate alpha-mangostin for evaluation of its inhibitory activity towards SARS-CoV-2 main protease.

1.2. Research Objectives

The objectives of this research are as follows:

- i. To screen mangosteen pericarp extract along with selected Thai herbal extracts for SARS-CoV-2 main protease (3CL^{Pro}) inhibitory activity
- ii. To prepare and characterize alpha-mangostin loaded polymeric micelles
- iii. To evaluate SARS-CoV-2 main protease (3CL^{Pro}) inhibitory activity of alpha-mangostin loaded in polymeric micelles

1.3. Novelty of Research

Although several approaches have been reported to improve the solubility of alpha-mangostin and developed different types of nanocarriers with different types of polymers to overcome the limitation of alpha-mangostin, there has not been any study done before on Soluplus[®] polymeric micelles as the nanocarrier to incorporate alpha-mangostin. Hence, the novelty of this research is that the alpha-mangostin compound will be loaded into the polymeric micelles formulated with Soluplus[®] for the evaluation of SARS-CoV-2 main protease (3CL^{Pro}) inhibitory activity of alpha-mangostin.

1.4. Research Hypothesis

Herbal extracts can inhibit SARS-CoV-2 main protease (3CL^{Pro}) activity, and alpha-mangostin can be encapsulated with high efficiency in polymeric micelles for evaluation of its inhibitory activity towards SARS-CoV-2 main protease (3CL^{Pro}).

CHAPTER 2. LITERATURE REVIEW

2.1. Potential SARS-CoV-2 main protease (3CL^{Pro}) inhibitory activity from herbal extracts

The COVID-19 disease that emerged in December 2019 is caused by SARS-CoV-2 virus (1). It is a single stranded positive-sense ribonucleic acid (RNA) enveloped virus (1). The replication of SARS-CoV-2 virus enormously depends on main protease, which is also known as 3-chymotrypsin-like protease (3CL^{Pro}) (4). It is a cysteine protease that has a three-domains structure with highly conserved binding pocket at four sub-sites to cleave polyproteins involved in viral replication process (Figure 1) (26).

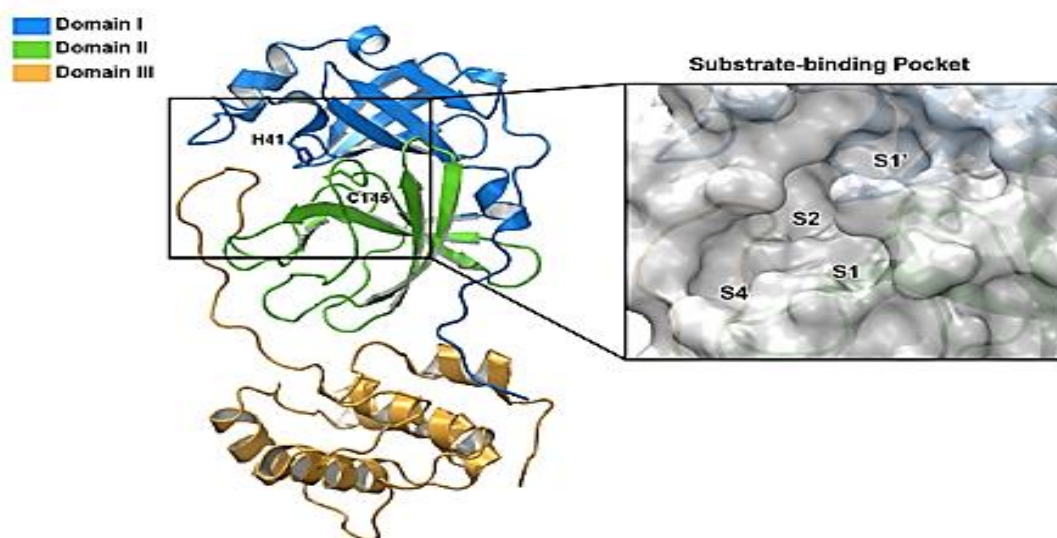


Figure 1. Structure of SARS-CoV-2 main protease (3CL^{Pro}) with substrate binding pocket

(Adapted from reference (26) under the copyright guideline of CC-BY license version 4.0 attached in Appendices)

The most interesting feature of 3CL^{Pro} is that it does not have human homolog, and hence it could be the promising druggable target (26). Since the comprehensive

level of health care against COVID-19 needs both vaccination and treatment, there is a current FDA authorized only for emergency use anti-viral treatment in adults and children over 12 years old. It is a combination of Nirmatrelvir and Ritonavir in an oral dosage form under Paxlovid® brand (27). Although Paxlovid® inhibits viral main protease (3CL^{Pro}) that is vital for viral replication, it has adverse effects and also possible interactions with many drugs metabolized by CYP450 enzymes (27, 28). Traditional herbal medicines have been used for many years as safe and effective treatments in various diseases, including viral infections (3). Hence, the discovery and development of natural product-based 3CL^{Pro} inhibitors could be one of the most promising strategies.

Some of the Thai herbs have been recently investigated with a favourable SARS-CoV-2 main protease (3CL^{Pro}) inhibitory activity. Bahun et al. reported that curcumin, which is a curcuminoid, isolated from the rhizome of turmeric (*Curcuma longa* Linn.) exhibited *in vitro* SARS-CoV-2 main protease (3CL^{Pro}) inhibitory activity with an IC₅₀ value of 11.9 ± 2.2 μ M (6). As mentioned in the study done by Wansri et al., piperine, which is an alkaloid, found from the extract of black pepper (*Piper nigrum* Linn.) fruits showed *in vitro* SARS-CoV-2 main protease (3CL^{Pro}) inhibitory activity at IC₅₀ of 178.4 ± 1.2 μ M (8). In addition, van de Sand et al. described that glycyrrhizin, which is a major phytochemical from the root of licorice (*Glycyrrhiza glabra* Linn.) had potent *in vitro* 3CL^{Pro} inhibitory effect by reduction of 70.3% protease activity at 30 μ M concentration of glycyrrhizin (7). Rutin, which is a naturally derived flavonoid from the extract of citrus peel (*Citrus hystrix* D.C.) has also been reported as the potential 3CL^{Pro} inhibitor with an IC₅₀ value of 325.6 ± 1.2 μ M (8). According to Rahman et al., rutin blocked the catalytic centre by forming the

strong fit to the binding pocket via hydrogen bond with cysteine 145 (Cys 145) located between the domain 1 and domain 2 of 3CL^{Pro} (Figure 2) (29).



Figure 2. The binding pattern of rutin with conserved substrate-binding pocket of 3CL^{Pro}

(Adapted from reference (29) under the copyright guideline of CC-BY license version 4.0 attached in Appendices)

2.2. Pharmacological activities and potential SARS-CoV-2 main protease (3CL^{Pro}) inhibitory activity of alpha-mangostin

Alpha-Mangostin is the major xanthone which is isolated from the extract of mangosteen pericarp. It has the highest yield of 78% by weight from the dry pericarp extract (30).

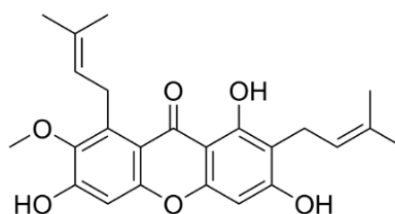


Figure 3. Chemical structure of alpha-mangostin

A wide range of pharmacological properties of alpha-mangostin have been reported including anti-oxidant, anti-cancer, anti-inflammatory, anti-bacterial and anti-viral activities (11). Pérez-Rojas et al. evaluated the anti-oxidant property of alpha-mangostin in a concentration-dependent study, and the results revealed the ability of alpha-mangostin in scavenging several reactive oxygen species as well as the formation of 3-nitropropionic acid (3-NP)-induced reactive oxygen species for renoprotective effect (12). Moreover, the anti-cancer property of alpha-mangostin has been discussed in the study done by Hung et al. in which alpha-mangostin inhibited matrix metalloproteinase-2/9 and urokinase-plasminogen expression through the c-Jun-N-terminal kinase (JNK) signaling pathway to suppress human prostate carcinoma cell (PC-3) metastasis (13). As mentioned by Chen et al., alpha-mangostin showed anti-inflammatory effect in carrageenan-induced paw oedema in mice by inhibiting the lipopolysaccharide-stimulated nitric oxide production (14). Furthermore, Suksamrarn et al. reported the strong inhibitory effect of alpha-mangostin against *Mycobacterium tuberculosis* in their study to examine the anti-tuberculosis potential (15). In addition, alpha-mangostin exhibits the potent anti-viral activity against a variety of human pathogenic viruses such as- hepatitis C virus (HCV), human immuno deficiency virus (HIV) and dengue virus (DENV) by inhibiting the replication of virus (16).

Recently, the potential SARS-CoV-2 main protease inhibitory activity of alpha-mangostin has been investigated. Due to the genomic similarity level of 67.5% between HIV protease and SARS-CoV-2 main protease, alpha-mangostin has the potential to be used as an inhibitor for SARS-CoV-2 main protease (17). This was supported by Hidayat et al. in their *in silico* study in which the inhibition of SARS-

CoV-2 main protease by alpha-mangostin was discussed (18). Similarly, Pyae et al. evaluated the binding mechanism and interaction of alpha-mangostin against SARS-CoV-2 main protease by using the fragment molecular orbital method (9). It was likely that the binding pattern of core structure of alpha-mangostin fits into the same binding pocket of main protease active site via $\pi - \pi$ interactions (Figure 4) (9).

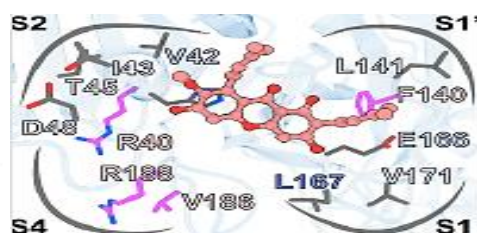


Figure 4. Interaction profile of alpha-mangostin (red structure) at the binding pocket of main protease active site

(Adapted from reference (9) under the copyright guideline of CC-BY license version 4.0 attached in Appendices)

However, alpha-mangostin is a hydrophobic compound with low aqueous solubility which undermines its bioavailability. To overcome this limitation, the development of alpha-mangostin loaded nanocarrier could be the feasible strategy (19).

2.3. Soluplus® polymeric micelles as the promising nanocarrier for hydrophobic compounds

Polymeric micelles are the suitable nanocarriers to incorporate hydrophobic bioactive compounds. Micelles belong to the dispersed colloidal systems, and they are considered as nano-sized colloidal dispersions (23). The robust core-shell structure of micelles and their intrinsic ability to improve the solubility of

hydrophobic compounds are the key characteristics of micelles. Moreover, the simple preparation method of polymeric micelles and the easy scalability at commercial/industrial level are the favorable features (23). In addition, polymeric micelles are able to efficiently encapsulate hydrophobic compounds and deliver them to the targeted site in the body (23).

Soluplus[®] is an amphiphilic polyvinyl caprolactam-polyvinyl acetate-polyethylene glycol graft copolymer with hydrophilic backbone and hydrophobic core which are made up of 13% polyethylene glycol (PEG), and 57% polyvinyl caprolactam with 30% polyvinyl acetate side chains by molecular weight respectively (31).

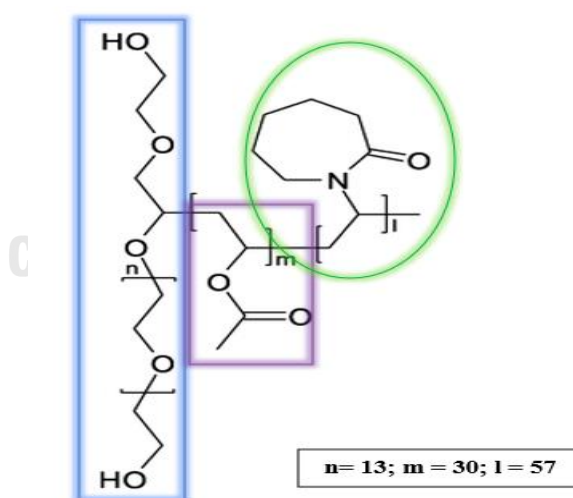


Figure 5. Chemical Structure of Soluplus[®]

In the self-assembly process of Soluplus[®] micelles, the hydrophobicity of copolymers acts as the main driving force to confine the hydrophobic part (polyvinyl caprolactam-polyvinyl acetate) to the core while the hydrophilic part (polyethylene glycol) is arranged in the shell region (Figure 6).

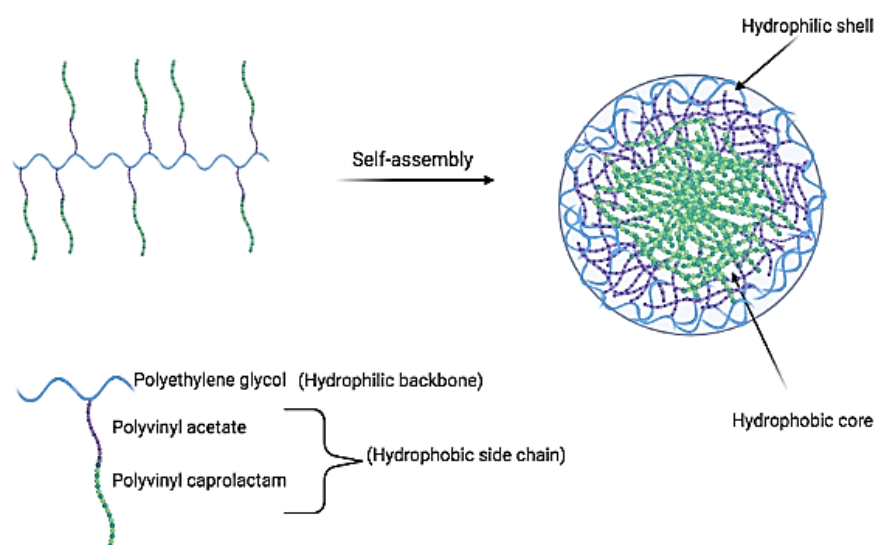


Figure 6. Self-assembly process of Soluplus[®] micelles

2.3.1. Significance of Soluplus[®] in development of polymeric micelles

The excellent solubilizing property as well as biocompatibility and biodegradability are the significant attributes of Soluplus[®] in the development of polymeric micelles for targeted delivery of hydrophobic drugs and compounds for potential applications in humans. In a study done by Pignatello et al., it was reported that Soluplus[®] polymeric micelles has the ability to improve the solubility of Biopharmaceutics Classification System (BCS) Class II drugs with low solubility (23). This was supported by Alopaesus et al. in their study to investigate the Soluplus[®] based system for oral delivery of Furosemide-loaded polymeric micelles. Based on

their study, the suitability of Soluplus[®] polymeric micelles as the nanocarrier for oral delivery of poorly soluble drugs was evident (25). In addition to oral delivery, Soluplus[®] polymeric micelles can be considered as the good candidate for intravenous drug delivery in cancer treatment. Jin et al. discussed in their study that fabrication of Soluplus[®] polymeric micelles loaded with anti-cancer drug, Fenbendazole (FEN) showed good *in vitro* drug release profile with no severe *in vivo* toxicity (32). Furthermore, Varela-Garcia et al. described the advantages of using Soluplus[®] polymeric micelles in ocular delivery of Acyclovir which is a poor aqueous soluble drug. The results showed that Soluplus[®] polymeric micelles enhanced the accumulation of drug with higher steady state flux at the targeted posterior eye segment (33). Moreover, Grotz et al. demonstrated the use of Soluplus[®] polymeric micelles as inhalable nanocarrier in pulmonary delivery of hydrophobic drug (Rifampicin) for potential treatment of tuberculosis. The *in vitro* aerodynamic results indicated a sustained drug release profile with improved microbicidal activity (34).

Soluplus[®] polymeric micelles can be used to encapsulate not only chemically synthetic hydrophobic drugs but also natural bioactive compounds with poor aqueous solubility. This was highlighted by Dian et al. in their study to improve the oral bioavailability and therapeutic efficacy of quercetin compound by encapsulating in Soluplus[®] polymeric micelles (35). Hence, Soluplus[®] polymeric micelles can be considered as the potential nanocarrier for alpha-mangostin to improve its pharmacological activity.

In addition to its potential as a nanocarrier to improve the solubility and bioavailability of hydrophobic compounds/drugs, Soluplus[®] polymeric micelles has

the specific desirable qualities to be used in pulmonary delivery of hydrophobic drugs/compounds via nasal administration. Firstly, the presence of hydrophilic PEG in Soluplus[®] structure promotes high circulation and the stability of drug-loaded polymeric micelles in circulation through the highly vascularized nasal mucosa (36). Moreover, the small particle size of less than 200 nm and the monodisperse distribution with the polydispersity index of less than 0.3 are the important parameters of Soluplus[®] polymeric micelles to avoid the engulfment of alveolar macrophages, and to achieve the uniform drug absorption profile across the pulmonary mucosal barriers respectively (36). Furthermore, the negative surface charge of Soluplus[®] polymeric micelles as characterized by zeta-potential can facilitate the penetration of pulmonary mucus layer for paracellular transport or transcytosis mechanism (36). However, the limitation is that there has not been any clinical data available yet for the use of Soluplus[®] in pulmonary delivery applications in humans.

Regarding the safety of Soluplus[®] for nanoformulation, Soluplus[®] is generally regarded as a safe pharmaceutical excipient with biocompatible and biodegradable properties. It is an approved pharmaceutical excipient in Europe by German Federal Ministry for Drugs and Medical Devices (37). It has been disclosed by the BASF manufacturer that doses of up to 8000 mg of Soluplus[®] in a healthy adult is considered to be safe according to their toxicological assessment in their clinical phase 1 trial (37). Moreover, Sipos et al. reported that the toxicity potential of Soluplus[®] is low which is $LD_{50(oral)} > 5000$ mg/kg (36). It was also announced in December 2022 that US FDA has accepted Soluplus[®] as a novel pharmaceutical excipient for evaluation of its safety in clinical trials (38).

In terms of stability of Soluplus[®] nanoformulation, Soluplus[®] is a suitable pharmaceutical excipient for promoting the stability of nanoformulation. This was supported by Rani et al. in their study for the stability enhancement of the encapsulated hydrophobic bioactive compound (curcumin) in Soluplus[®] polymeric micelles (39). It was reported that the rate of degradation of the encapsulated curcumin compound was less than 3% in a 3-day duration (39). Another study also showed the enhanced stability of nanosuspension formulated with Soluplus[®]. It was demonstrated that the stability of drug incorporated with Soluplus[®] was improved as compared to the drug itself (40). Most importantly, Pignatello et al. stated that the drug-loaded Soluplus[®] nanoformulation was stable at both room temperature and at 4°C storage conditions during their 6-month stability study (23).

In the formulation of Soluplus[®] polymeric micelles loaded with hydrophobic drugs/compounds (for example, alpha-mangostin), there are hydrophobic interactions between alpha-mangostin compound and the hydrophobic core structure of polymeric micelles for efficient encapsulation while the hydrophilic shell of polymeric micelles improves the stability and solubility of encapsulated alpha-mangostin compound. The increase in solubility of alpha-mangostin inside the nanomaterial improves its bioavailability, thereby enhancing its pharmacological activity. Since Soluplus[®] is biodegradable, the release of alpha-mangostin encapsulated inside the polymeric micelles can be achieved through the cleavage of chemical bonds within the polymeric matrix as well as at the surface of matrix due to dissolution (41).

CHAPTER 3. RESEARCH METHODOLOGY

3.1. Herbal materials

The herbal materials used in this research were purchased from Chaokrompoe Thai Traditional Medicine Store or collected from the garden of Faculty of Pharmaceutical Sciences, Chulalongkorn University, Bangkok, Thailand in January 2022. The identification of herbal materials was based on Thai Pharmacopoeia (42) and Plant Names of Thailand (43). The following table (**Table 1.**) shows the herbal materials used in this research.

Table 1. List of selected herbal materials used for in vitro screening of 3CL^{Pro}

No.	Plant (Common Name)	Scientific Name	Family	Part Used
01	Nutgrass	<i>Cyperus rotundus</i> L.	Cyperaceae	Fruit
02	Sweet Basil	<i>Ocimum basilicum</i> L.	Lamiaceae	Leaf
03	Butterfly Pea	<i>Clitoria ternatea</i> L.	Fabaceae	Flower
04	Licorice	<i>Glycyrrhiza glabra</i> L.	Fabaceae	Root
05	Roselle	<i>Hibiscus sabdariffa</i> L.	Malvaceae	Stem
06	Mulberry	<i>Morus alba</i> L.	Moraceae	Leaf
07	Roselle	<i>Hibiscus sabdariffa</i> L.	Malvaceae	Leaf
08	Pennywort	<i>Centella asiatica</i> L.	Apiaceae	Leaf
09	Long Pepper	<i>Piper longum</i> L.	Piperaceae	Fruit
10	Long Pepper	<i>Piper longum</i> L.	Piperaceae	Leaf
11	Samphao	<i>Chaetocarpus castanocarpus</i> (Roxb.) Thwaites	Peraceae	Stem
12	Safflower	<i>Carthamus tinctorius</i> L.	Asteraceae	Flower
13	Paracress	<i>Acmella oleracea</i> (L.) R.K. Jansen	Asteraceae	Rhizome
14	Turmeric	<i>Curcuma longa</i> L.	Zingiberaceae	Rhizome
15	Ankol	<i>Alangium salviifolium</i> (L.f.) Wangerin	Cornaceae	Bark
16	Garden Cress	<i>Lepidium sativum</i> L.	Brassicaceae	Seed
17	Black Cumin	<i>Nigella sativa</i> L.	Ranunculaceae	Seed
18	Cumin	<i>Cuminum cyminum</i> L.	Apiaceae	Seed
19	Kaffir Lime	<i>Citrus hystrix</i> DC.	Rutaceae	Peel
20	Beleric Myrobalan	<i>Terminalia bellirica</i> (Gaertn.) Roxb.	Combretaceae	Fruit
21	Myrobalan	<i>Terminalia chebula</i> Retz.	Combretaceae	Fruit
22	Indian Gooseberry	<i>Phyllanthus emblica</i> L.	Phyllanthaceae	Fruit
23	Sweet Fennel	<i>Foeniculum vulgare</i> Mill	Apiaceae	Seed
24	Tamarind	<i>Tamarindus indica</i> L.	Fabaceae	Leaf
25	Ginger	<i>Zingiber officinale</i> Roscoe	Zingiberaceae	Rhizome
26	Heart-leaved Moonseed	<i>Tinospora crispa</i> (L.) Miers ex Hook.f. & Thomson	Menispermaceae	Stem
27	Dill	<i>Anethum graveolens</i> L.	Apiaceae	Seed
28	Mangosteen	<i>Garcinia mangostana</i> L.	Clusiaceae	Fruit

3.2. Chemicals and reagents

Soluplus[®] was received as a gift from BASF (Thailand). All HPLC grade solvents were purchased from Merck (Darmstadt, Germany). Chemicals were purchased from Sigma-Aldrich (Missouri, USA).

3.3. Preparation of herbal extracts

The pericarp of mangosteen fruit and the other 27 randomly selected herbal materials were cleaned with tap water and dried in a hot-air oven at 50°C for 48 hours. Each dried sample was ground by a hammer milling machine under 5 mm screen sieve to obtain 500 g of coarse powder form which was then sealed in the muslin cloth bag and immersed in the glass jar with 2 L of methanol for 7 days at room temperature for maceration process. Maceration was repeated for another 2 times. After that, the combined methanolic crude extracts of each herbal material was concentrated under reduced pressure by using a rotary evaporator (Rotavapor[®] R-100, Büchi) to get the semi-solid crude extract. Finally, the extract was dried under high vacuum for 1 hour. The amount of 10 mg of each extract was kept in an eppendorf at -20°C until use.

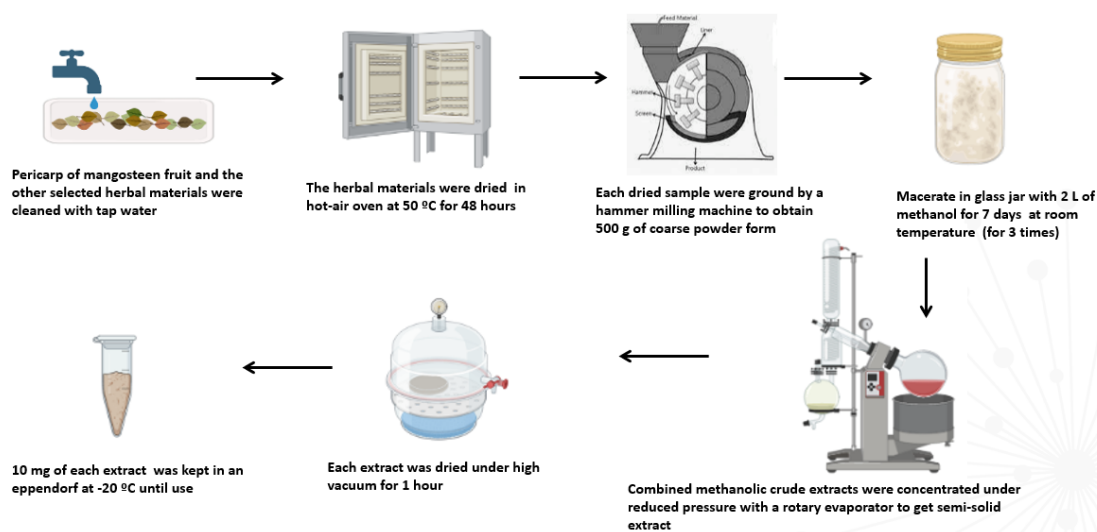


Figure 7. Preparation of herbal extracts

3.4. Screening of mangosteen pericarp extract along with selected Thai herbal extracts for SARS-CoV-2 main protease (3CL^{Pro}) inhibitory activity

In order to screen the mangosteen pericarp extract and the other 27 selected herbal extracts, 0.1 mg/mL of each extract was prepared in dimethyl sulfoxide (DMSO). DMSO is a frequently used organic solvent for *in vitro* biological assay of natural products due to its non-toxicity characteristic and stability at high temperatures. 3CL^{Pro} inhibitory assay was performed cost effectively with the recombinant 3CL^{Pro} from *Escherichia coli* bacteria. The fluorogenic substrate E (EDANS) TSAVLQSGFRK (DABCYL) at the concentration of 25 μ M was used to perform the assay with 0.2 μ M 3CL^{Pro} in the presence of phosphate buffer solution, 1.0 mM dithiothreitol (DTT) and 2% DMSO at the fixed reaction volume of 100 μ L. The fluorescence signals at the excitation wavelength of 340 nm and the emission wavelength of 490 nm were measured by using a microplate reader. The analysis of inhibitory activity results of herbal extracts was conducted with the initial rates of

blank compound without the inhibitor and 100 μM of rutin as a positive control. Rutin was used as a positive control due to its potential 3CL^{Pro} inhibitory activity, cost effectiveness, and easy accessibility in Thailand as compared to the other commercially available test compounds.

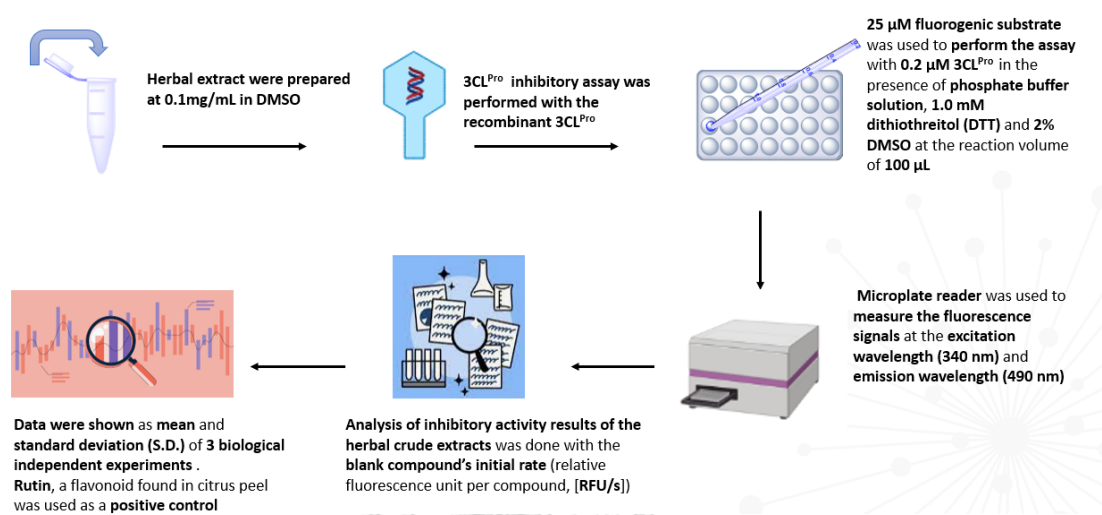


Figure 8. Screening of mangosteen pericarp extract along with selected Thai herbal extracts for SARS-CoV-2 main protease (3CL^{Pro}) inhibitory activity

3.5. Preparation of alpha-mangostin loaded polymeric micelles

Alpha-mangostin loaded polymeric micelles were developed with Soluplus[®] (Figure 9). Soluplus[®] is an amphiphilic graft copolymer which is made up of polyethylene glycol as the hydrophilic backbone, and polyvinyl caprolactam with polyvinyl acetate side chains as the hydrophobic core. Hence, the hydrophobic alpha-mangostin compound was loaded in the hydrophobic core of Soluplus[®] polymeric micelles. First of all, different concentrations of alpha-mangostin loaded polymeric micelles such as 2.5% w/w, 5% w/w and 10% w/w formulations were prepared with Soluplus[®] at the concentration of 1 mg/mL by using a thin-film hydration method.

Since 5% w/w formulation showed the most promising results, further preparations of alpha-mangostin loaded polymeric micelles were conducted with higher concentrations of Soluplus[®] at 2 mg/mL, 4 mg/mL and 10 mg/mL.

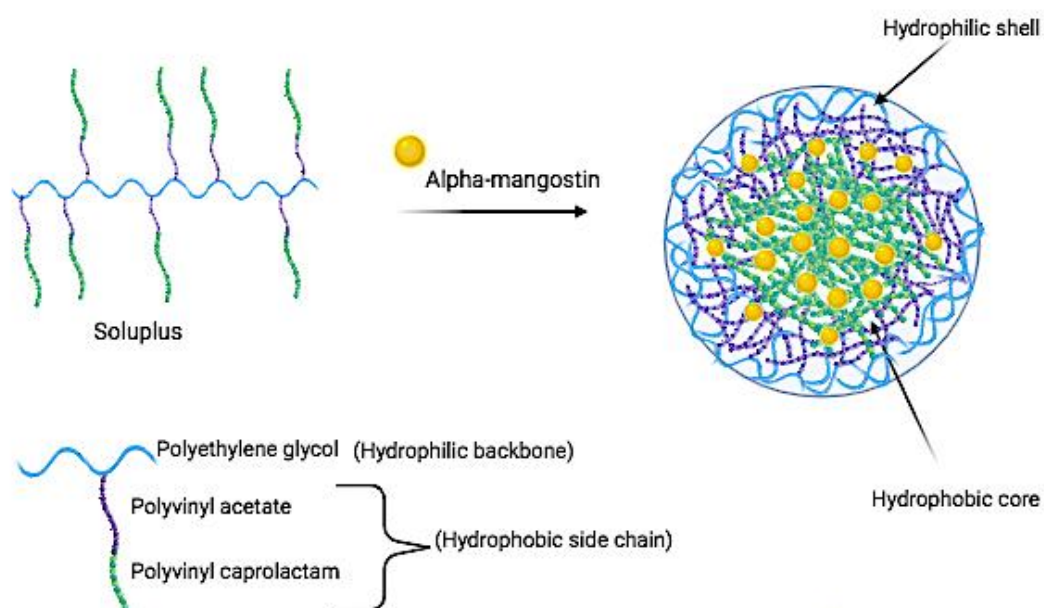


Figure 9. Alpha-mangostin loaded Soluplus[®] polymeric micelles

3.5.1. Preparation of 2.5% w/w alpha-mangostin loaded polymeric micelles with Soluplus[®] concentration of 1 mg/mL

0.5 mg of alpha-mangostin and 20 mg of Soluplus[®] were dissolved in 20 mL of HPLC grade methanol in 250 mL rotary evaporator flask. The mixture was concentrated under reduced pressure by rotary evaporator (Rotavapor[®] R-100, Büchi) at 200 bar for 20 minutes at 70°C to obtain a thin film of polymer. After that, 20 mL of ultrapure water kept at 70°C was added to hydrate the film, and continuously rotated at 250 rpm to form polymeric micelles. This was followed by sonication in water bath for 3 minutes to reduce the particles size. The non-incorporated alpha-mangostin was separated by syringe filtration through a 0.45 µm cellulose acetate

membrane syringe filter. As a result, the filtrate of alpha-mangostin loaded Soluplus[®] polymeric micelles were obtained.

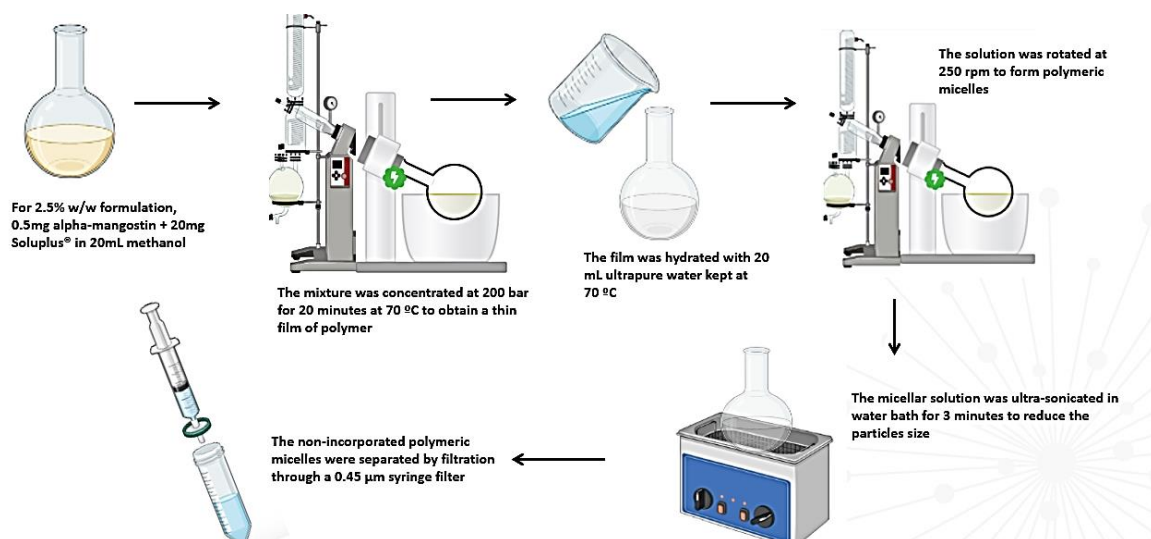


Figure 10. Preparation of 2.5% w/w alpha-mangostin loaded polymeric micelles with Soluplus[®] concentration of 1 mg/mL

3.5.2. Preparation of 5% w/w alpha-mangostin loaded polymeric micelles with Soluplus[®] concentration of 1 mg/mL

1 mg of alpha-mangostin and 20 mg of Soluplus[®] were dissolved in 20 mL of HPLC grade methanol in 250 mL rotary evaporator flask. The mixture was concentrated under reduced pressure by rotary evaporator (Rotavapor[®] R-100, Büchi) at 200 bar for 20 minutes at 70°C to obtain a thin film of polymer. After that, 20 mL of ultrapure water kept at 70°C was added to hydrate the film, and continuously rotated at 250 rpm to form polymeric micelles. This was followed by sonication in water bath for 3 minutes to reduce the particles size. The non-incorporated alpha-mangostin was separated by syringe filtration through a 0.45 µm cellulose acetate

membrane syringe filter. As a result, the filtrate of alpha-mangostin loaded Soluplus[®] polymeric micelles were obtained.

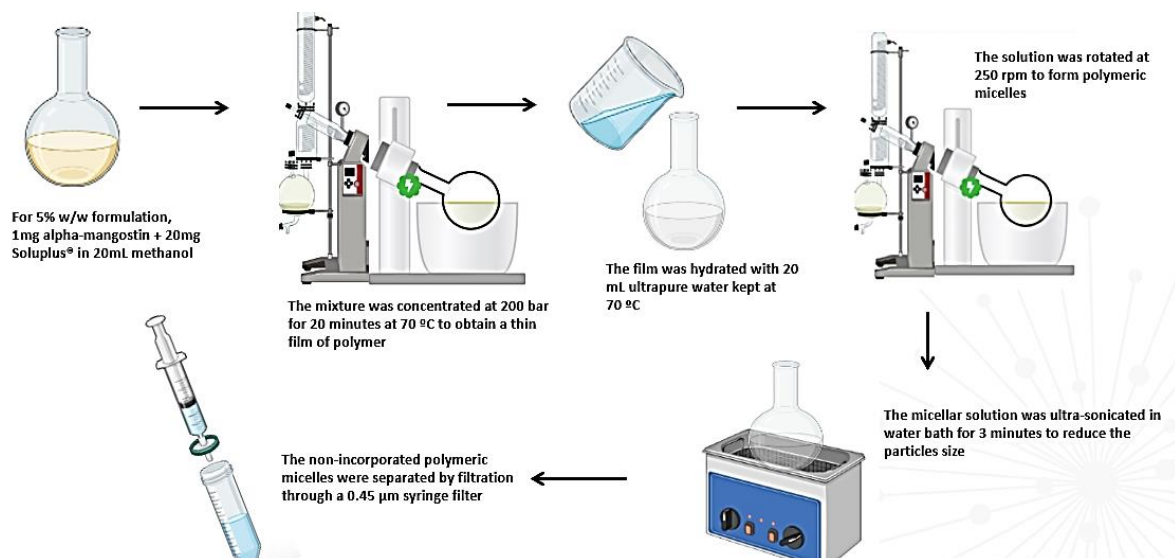


Figure 11. Preparation of 5% w/w alpha-mangostin loaded polymeric micelles with Soluplus[®] concentration of 1 mg/mL

3.5.3. Preparation of 10% w/w alpha-mangostin loaded polymeric micelles with Soluplus[®] concentration of 1 mg/mL

2 mg of alpha-mangostin and 20 mg of Soluplus[®] were dissolved in 20 mL of HPLC grade methanol in 250 mL rotary evaporator flask. The mixture was concentrated under reduced pressure by rotary evaporator (Rotavapor[®] R-100, Büchi) at 200 bar for 20 minutes at 70°C to obtain a thin film of polymer. After that, 20 mL of ultrapure water kept at 70°C was added to hydrate the film, and continuously rotated at 250 rpm to form polymeric micelles. This was followed by sonication in water bath for 3 minutes to reduce the particles size. The non-incorporated alpha-mangostin was separated by syringe filtration through a 0.45 µm cellulose acetate

membrane syringe filter. As a result, the filtrate of alpha-mangostin loaded Soluplus® polymeric micelles were obtained.

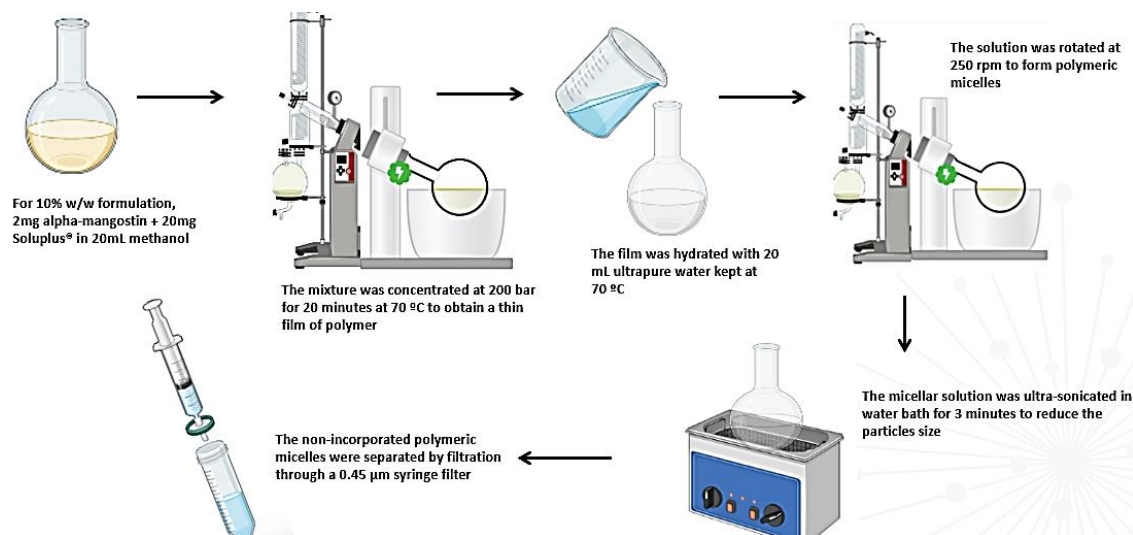


Figure 12. Preparation of 10% w/w alpha-mangostin loaded polymeric micelles with Soluplus® concentration of 1 mg/mL

3.5.4. Preparation of 5% w/w alpha-mangostin loaded polymeric micelles with Soluplus® concentration of 2 mg/mL

2 mg of alpha-mangostin and 40 mg of Soluplus® were dissolved in 20 mL of HPLC grade methanol in 250 mL rotary evaporator flask. The mixture was concentrated under reduced pressure by rotary evaporator (Rotavapor® R-100, Büchi) at 200 bar for 20 minutes at 70°C to obtain a thin film of polymer. After that, 20 mL of ultrapure water kept at 70°C was added to hydrate the film, and continuously rotated at 250 rpm to form polymeric micelles. This was followed by sonication in water bath for 3 minutes to reduce the particles size. The non-incorporated alpha-mangostin was separated by syringe filtration through a 0.45 µm cellulose acetate

membrane syringe filter. As a result, the filtrate of alpha-mangostin loaded Soluplus[®] polymeric micelles were obtained.

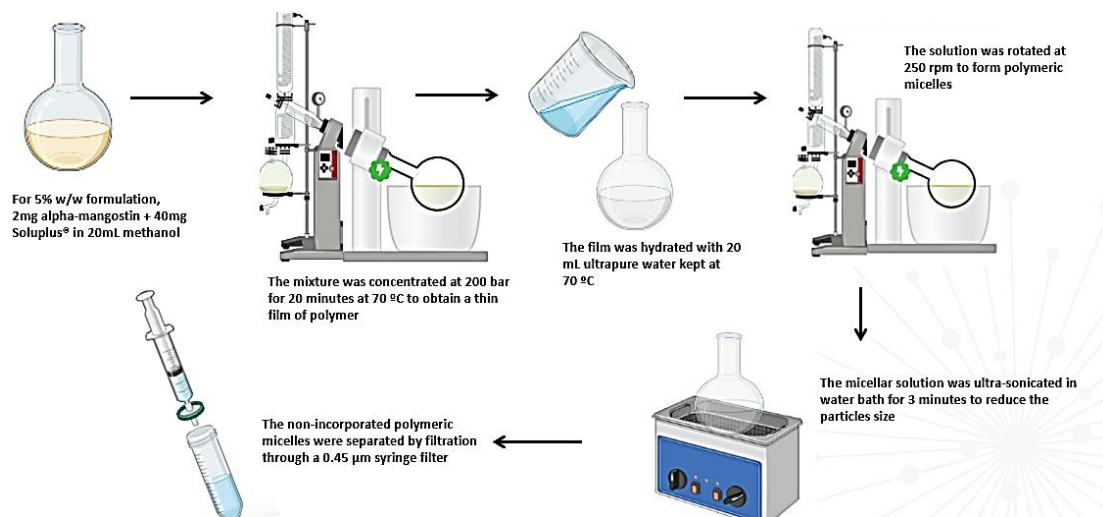


Figure 13. Preparation of 5% w/w alpha-mangostin loaded polymeric micelles with Soluplus[®] concentration of 2 mg/mL

3.5.5. Preparation of 5% w/w alpha-mangostin loaded polymeric micelles with Soluplus[®] concentration of 4 mg/mL

4 mg of alpha-mangostin and 80 mg of Soluplus[®] were dissolved in 20 mL of HPLC grade methanol in 250 mL rotary evaporator flask. The mixture was concentrated under reduced pressure by rotary evaporator (Rotavapor[®] R-100, Büchi) at 200 bar for 20 minutes at 70°C to obtain a thin film of polymer. After that, 20 mL of ultrapure water kept at 70°C was added to hydrate the film, and continuously rotated at 250 rpm to form polymeric micelles. This was followed by sonication in water bath for 3 minutes to reduce the particles size. The non-incorporated alpha-mangostin was separated by syringe filtration through a 0.45 µm cellulose acetate membrane syringe filter. As a result, the filtrate of alpha-mangostin loaded Soluplus[®] polymeric micelles were obtained.

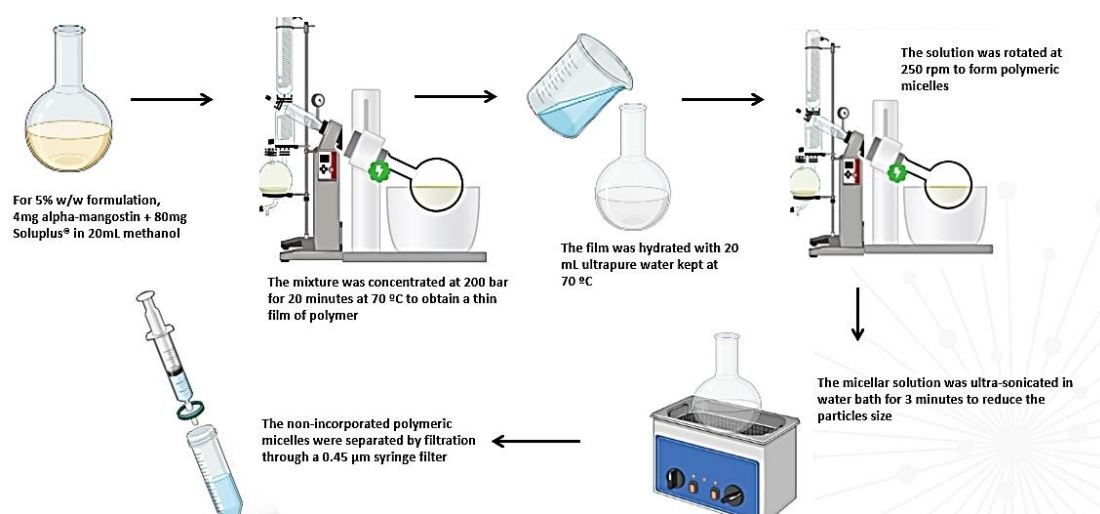


Figure 14. Preparation of 5% w/w alpha-mangostin loaded polymeric micelles with Soluplus[®] concentration of 4 mg/mL

3.5.6. Preparation of 5% w/w alpha-mangostin loaded polymeric micelles with Soluplus[®] concentration of 10 mg/mL

5 mg of alpha-mangostin and 100 mg of Soluplus[®] were dissolved in 10 mL of HPLC grade methanol in 250 mL rotary evaporator flask. The mixture was concentrated under reduced pressure by rotary evaporator (Rotavapor[®] R-100, Büchi) at 200 bar for 20 minutes at 70 °C to obtain a thin film of polymer. After that, 10 mL of ultrapure water kept at 70 °C was added to hydrate the film, and continuously rotated at 250 rpm to form polymeric micelles. This was followed by sonication in water bath for 3 minutes to reduce the particles size. The non-incorporated alpha-mangostin was separated by syringe filtration through a 0.45 µm cellulose acetate membrane syringe filter. As a result, the filtrate of alpha-mangostin loaded Soluplus[®] polymeric micelles were obtained.

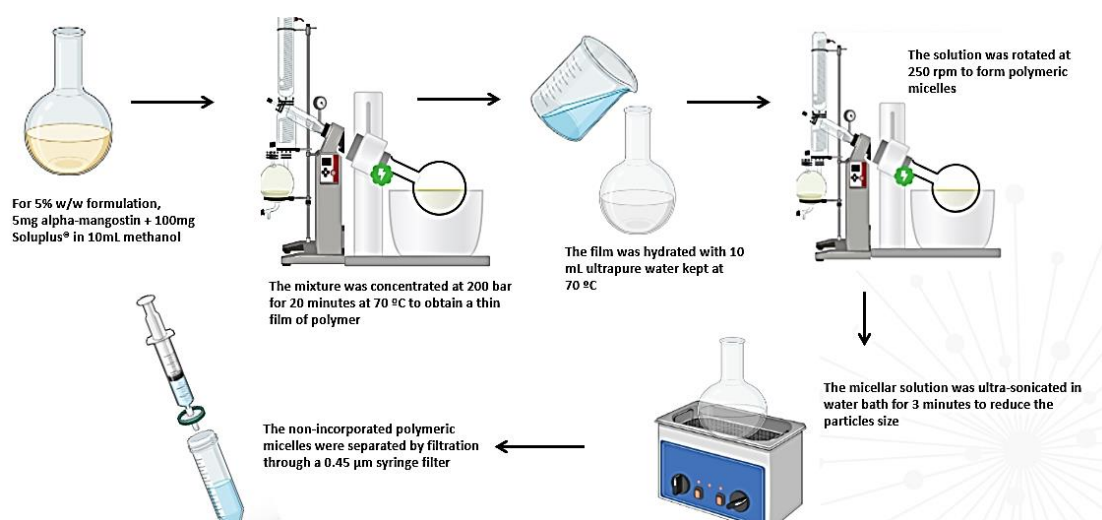


Figure 15. Preparation of 5% w/w alpha-mangostin loaded polymeric micelles with Soluplus® concentration of 10 mg/mL

3.6. Determination of encapsulation efficiency and loading capacity

The encapsulation efficiency (%EE) and loading capacity (%LC) of alpha-mangostin loaded Soluplus® polymeric micelles were analyzed and determined by using UV-vis spectrophotometer and high performance thin layer chromatography (HPLC) technique.

The preliminary analyses of encapsulation efficiency (%EE) and loading capacity (%LC) of 2.5% w/w, 5% w/w and 10% w/w alpha-mangostin loaded polymeric micelles at Soluplus® concentration of 1 mg/mL were undertaken with UV-vis spectrophotometer.

3.6.1. Separation of non-incorporated/non-encapsulated alpha-mangostin

After the preparation of alpha-mangostin loaded polymeric micelles, the non-incorporated/non-encapsulated alpha-mangostin components were separated by syringe filtration through a 0.45 µm cellulose acetate membrane syringe filter. This is

because syringe filtration is a simple and time-efficient method for the removal of non-incorporated/non-encapsulated alpha-mangostin. The pore size of 0.45 μm membrane filter only allows to pass through the alpha-mangostin encapsulated in polymeric micelles with size smaller than 0.45 μm . The non-incorporated/non-encapsulated alpha-mangostin with size larger than 0.45 μm were retained on the filter. Also, the filter is made up of cellulose acetate membrane that is hydrophilic. This would facilitate to obtain the alpha-mangostin encapsulated in polymeric micelles with hydrophilic shell. Since alpha-mangostin is hydrophobic, any non-incorporated/non-encapsulated alpha-mangostin were retained on the filter. As a result, the filtrate of alpha-mangostin loaded Soluplus[®] polymeric micelles were obtained to determine % encapsulation efficiency and % loading capacity.

3.6.2. Evaluation of % encapsulation efficiency and % loading capacity by UV

The UV quantitative analysis of alpha-mangostin content, and the preparation of standard calibration curve were based on the protocol from a previous study with slight modifications (44). The UV analysis was performed with UV-vis Evolution 300 ThermoFisher Scientific[™] at 320 nm wavelength by using a 1.0 cm quartz cell to measure the absorbance of standard solutions at final concentrations of 10, 8, 6, 4, 2 $\mu\text{g}/\text{mL}$. After that, 2 mL of alpha-mangostin loaded polymeric micelles were diluted with HPLC grade methanol in 10 mL volumetric flask. The UV absorbance of each formulation was measured by using a 1.0 cm quartz cell at 320 nm wavelength for %EE and %LC analyses.

3.6.3. Evaluation % encapsulation efficiency and % loading capacity by HPLC

The HPLC quantitative analysis of alpha-mangostin content, and the preparation of standard curve for HPLC were undertaken according to the protocol from a previous study with slight modifications (45). HPLC analysis was performed on an Agilent™ 1260 Infinity II HPLC system which is equipped with a quaternary pump, an UV vis detector, an auto sampler and a C18 column with a C18 guard cartilage column. The mobile solvents used were 0.1% v/v acetic acid in ultrapure water (solvent A) and acetonitrile (solvent B). The sample injection volume was 10 µL and the flow rate was 1 mL/min. Total running time was 37 minutes at 25°C column temperature at UV-vis detector wavelength of 320 nm. The standard curve was plotted based on the peak areas of standard solutions at final concentrations of 200, 100, 50, 25, 10 µg/mL. After that, 2 mL of alpha-mangostin loaded polymeric micelles of each formulation was diluted with HPLC grade methanol in 10 mL volumetric flask. The solution was filtered into the 1.5 mL HPLC amber glass vial by using a 0.45 µm cellulose acetate membrane syringe filter. Each formulation's peak area of curve was examined by HPLC for %EE and %LC analyses.

The encapsulation efficiency (%EE) and loading capacity (%LC) of alpha-mangostin loaded Soluplus® polymeric micelles of each formulation was calculated according to the equations as follows:

Encapsulation Efficiency (%EE)

$$= \frac{\text{Amount of } \alpha \text{ mangostin that can be encapsulated in polymeric micelles}}{\text{Amount of initial } \alpha \text{ mangostin}} \times 100\%$$

Loading Capacity (%LC)

$$= \frac{\text{Amount of } \alpha \text{ mangostin that can be encapsulated in polymeric micelles}}{\text{Amount of polymer} + \text{Amount of initial } \alpha \text{ mangostin}} \times 100\%$$

3.7. Characterization of alpha-mangostin loaded polymeric micelles

The particle size distributions in terms of hydrodynamic diameter, polydispersity index (PDI) as well as zeta potential of alpha-mangostin loaded Soluplus[®] polymeric micelles of each formulation were analyzed by dynamic light scattering (DLS) with Zetasizer Pro (Malvern[™]). Hydrodynamic diameter reflects how the particle size exhibits in an aqueous medium (46). Polydispersity index (PDI) measures the distribution of colloidal particles (47). A PDI value less than 0.1 is considered as good homogeneity while a PDI value between 0.1 and 0.3 indicates a narrow size distribution. Zeta potential is an electro-kinetic potential in colloidal dispersions. It is a measurable indicator of the stability of colloidal dispersions. Although the zeta potential values larger than +30 mV and -30 mV are preferably recognized for high stability of micelles, the zeta potential values larger than +10 mV and -10 mV can still be considered for incipient stability of micelles (48).

The morphology of both blank Soluplus[®] polymeric micelles and alpha-mangostin loaded Soluplus[®] polymeric micelles of the selected formulation was observed by transmission electron microscopy (TEM) with the microscope (JEM-1400) under negative staining with 2% uranyl acetate solution which is one of the commonly used staining reagents to give a satisfactory contrast in TEM images.

3.8. Stability study of alpha-mangostin loaded polymeric micelles

The stability study was performed according to the protocol from previous micelles stability studies with slight modifications (49, 50). Alpha-mangostin loaded Soluplus[®] polymeric micelles of the selected formulation was kept at two different temperatures (4°C and 25°C) in the 15 mL conical tubes for 30 days. The changes in terms of encapsulation efficiency (%EE), loading capacity (%LC), hydrodynamic diameter, polydispersity index and zeta-potential were examined at 0, 1, 3, 5, 7, 14 and 30 days.

3.9. Evaluation of SARS-CoV-2 main protease (3CL^{Pro}) inhibitory activity of alpha-mangostin in polymeric micelles

Alpha-mangostin compound dissolved in DMSO and alpha-mangostin loaded in Soluplus[®] polymeric micelles of the selected formulation were screened together to evaluate their inhibitory activity towards SARS-CoV-2 main protease (3CL^{Pro}). The screening protocol was the same as the protocol used in the screening of herbal extracts for SARS-CoV-2 main protease (3CL^{Pro}) inhibitory activity. The analysis of inhibitory activity results was conducted with the initial rates of blank compound without the inhibitor and 100 nM PF-07321332 as a positive control.

3.10. Evaluation of *in vitro* cytotoxicity of alpha-mangostin in polymeric micelles in HaCaT cells line

Alpha-mangostin compound dissolved in DMSO and alpha-mangostin loaded in Soluplus[®] polymeric micelles of the selected formulation were evaluated for their *in vitro* cytotoxicity in HaCaT cells line by using 3-(4,5-dimethylthiazol-2-yl)-2,5-diphenyltetrazolium bromide (MTT) assay. HaCaT cells were cultivated in Dulbecco's Modified Eagle's Medium (DMEM) consisting of 10% Fetal Bovine Serum (FBS), 1% L-glutamine, and 1% antibiotics in T25 flasks and incubated at

37°C under 5% CO₂ atmosphere for 48 hours. When the cells were developed almost 80% confluency, the cells were subcultured and incubated for 48 hours.

Cells were seeded at the density of 5×10^3 cells/well in 96 well plates and let the cells to attach the plates for 24 hours. After that, cells were treated with both alpha-mangostin compound dissolved in DMSO (without the nanocarrier) and alpha-mangostin loaded in Soluplus[®] polymeric micelles in serial dilutions at the concentrations of 100, 50, 25, 10, 5, 2.5, 1 µg/mL. DMEM was used as a negative control. After 24 hours of treatment and incubation at 37°C under 5% CO₂ atmosphere, the medium was removed. The cell viability was determined by adding 100 µL of MTT solution (0.5 mg/mL). The 96 well plates were incubated at 37°C for 3 hours under light protection. The supernatant solution was carefully removed and 100 µL of DMSO was added to each well to dissolve the purple formazan crystals. The absorbance was measured by using a microplate reader at 570 nm and % cell viability was calculated.

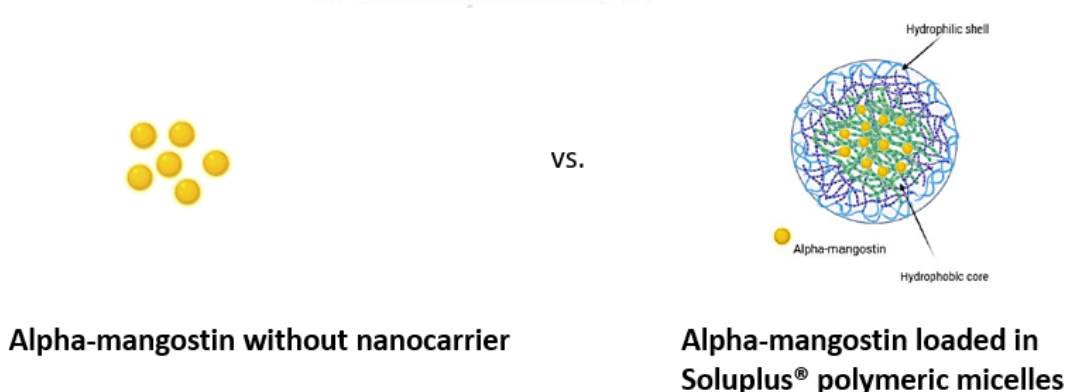


Figure 16. Evaluations of SARS-CoV-2 main protease (3CL^{Pro}) inhibitory activity and *in vitro* cytotoxicity of alpha-mangostin without nanocarrier and alpha-mangostin loaded in polymeric micelles

3.11. Data analysis

Each test in this study was performed in triplicate. Data were presented as mean \pm standard deviation (S.D.) of three independent experiments. One-way analysis of variance (ANOVA) was used for statistical analysis with GraphPad Prism 9.3.1 (San Diego, CA, USA), and a p-value < 0.05 was considered as statistically significant.



CHAPTER 4. RESULTS AND DISCUSSION

4.1. Screening of mangosteen pericarp extract along with 27 herbal extracts for SARS-CoV-2 main protease (3CL^{Pro}) inhibitory activity

The results of the *in vitro* 3CL^{Pro} inhibitory activity screening of mangosteen pericarp extract and the randomly selected 27 herbal crude extracts at 0.1 mg/mL were presented in **Table 2** and **Figure 17**. Among all the herbal extracts, licorice root (H04), long pepper fruits (H09), turmeric rhizome (H14), sweet fennel seeds (H23) and mangosteen fruit pericarp showed significant inhibition of 3CL^{Pro} activity with residual protease activities of 33.9%, 54.2%, 13.1%, 50.7% and 5.15% respectively, while rutin possessed 60.3%. The lower the residual percent (%) protease activity, the higher the inhibition of the 3CL^{Pro} activity of the herbal extracts. It was observed that the extract from mangosteen pericarp has the highest inhibition of 3CL^{Pro} activity which was followed by the extract of turmeric rhizome and the extract from licorice root. The extracts from sweet fennel seeds and long pepper fruits displayed similar % inhibition. The *in vitro* screening results of mangosteen fruit pericarp, licorice root (H04), long pepper fruits (H09), turmeric rhizome (H14) and sweet fennel seeds (H23) showed significant inhibition of 3CL^{Pro} activity, which were more potent than that of rutin (**Figure 18**).

Table 2. *In vitro* SARS-CoV-2 main protease (3CL^{Pro}) inhibition of herbal extracts at 0.1 mg/mL

No.	Common Name	Scientific Name	Family	Part Used	% Protease Activity \pm S.D. ^a
H01	Nutgrass	<i>Cyperus rotundus</i> L.	Cyperaceae	Fruit	75.1 \pm 1.4****
H02	Sweet Basil	<i>Ocimum basilicum</i> L.	Lamiaceae	Leaf	108.4 \pm 4.1
H03	Butterfly Pea	<i>Clitoria ternatea</i> L.	Fabaceae	Flower	100.3 \pm 0.3
H04	Licorice	<i>Glycyrrhiza glabra</i> L.	Fabaceae	Root	33.9 \pm 1.1****
H05	Roselle	<i>Hibiscus sabdariffa</i> L.	Malvaceae	Stem	98.9 \pm 2.2
H06	Mulberry	<i>Morus alba</i> L.	Moraceae	Leaf	83.8 \pm 4.1****
H07	Roselle	<i>Hibiscus sabdariffa</i> L.	Malvaceae	Leaf	97.5 \pm 1.7
H08	Pennywort	<i>Centella asiatica</i> L.	Apiaceae	Leaf	94.6 \pm 0.4
H09	Long Pepper	<i>Piper longum</i> L.	Piperaceae	Fruit	54.2 \pm 3.3****
H10	Long Pepper	<i>Piper longum</i> L.	Piperaceae	Leaf	126.4 \pm 2.7****
H11	Samphao	<i>Chaetocarpus castanocarpus</i> (Roxb.) Thwaites	Peraceae	Stem	73.6 \pm 3.0****
H12	Safflower	<i>Carthamus tinctorius</i> L.	Asteraceae	Flower	134.5 \pm 4.4****
H13	Paracress	<i>Acmella oleracea</i> (L.) R.K. Jansen	Asteraceae	Rhizome	134.7 \pm 4.1****
H14	Turmeric	<i>Curcuma longa</i> L.	Zingiberaceae	Rhizome	13.1 \pm 0.5****
H15	Ankol	<i>Alangium salviifolium</i> (L.f.) Wangerin	Cornaceae	Bark	88.2 \pm 2.2**
H16	Garden Cress	<i>Lepidium sativum</i> L.	Brassicaceae	Seed	137.9 \pm 8.1****
H17	Black Cumin	<i>Nigella sativa</i> L.	Ranunculaceae	Seed	102.5 \pm 5.4
H18	Cumin	<i>Cuminum cyminum</i> L.	Apiaceae	Seed	99.1 \pm 5.0
H19	Kaffir Lime	<i>Citrus hystrix</i> DC.	Rutaceae	Peel	113.2 \pm 5.6****
H20	Beleric Myrobalan	<i>Terminalia bellirica</i> (Gaertn.) Roxb.	Combretaceae	Fruit	79.3 \pm 3.8****
H21	Myrobalan	<i>Terminalia chebula</i> Retz.	Combretaceae	Fruit	111.2 \pm 3.9**
H22	Indian Gooseberry	<i>Phyllanthus emblica</i> L.	Phyllanthaceae	Fruit	90.6 \pm 1.2*
H23	Sweet Fennel	<i>Foeniculum vulgare</i> Mill	Apiaceae	Seed	50.7 \pm 3.0****
H24	Tamarind	<i>Tamarindus indica</i> L.	Fabaceae	Leaf	68.2 \pm 0.9****
H25	Ginger	<i>Zingiber officinale</i> Roscoe	Zingiberaceae	Rhizome	131.2 \pm 1.4****
H26	Heart-leaved Moonseed	<i>Tinospora crispa</i> (L.) Miers ex Hook.f. & Thomson	Menispermaceae	Stem	112.6 \pm 2.5***
H27	Dill	<i>Anethum graveolens</i> L.	Apiaceae	Seed	61.5 \pm 3.9****
	Mangosteen	<i>Garcinia mangostana</i> L.	Clusiaceae	Fruit	5.15 \pm 0.64****
	Rutin ^b	-	-	-	60.3 \pm 2.4***

^a Protease activity was measured as the relative fluorescence unit per second, [RFU/s]. ^b Rutin (positive control) was tested at 100 μ M. The % protease activity of rutin and extracts were compared to that of blank compound without the inhibitor (negative control); *p<0.05, **p<0.001, ***p<0.0001 and ****p<0.00001

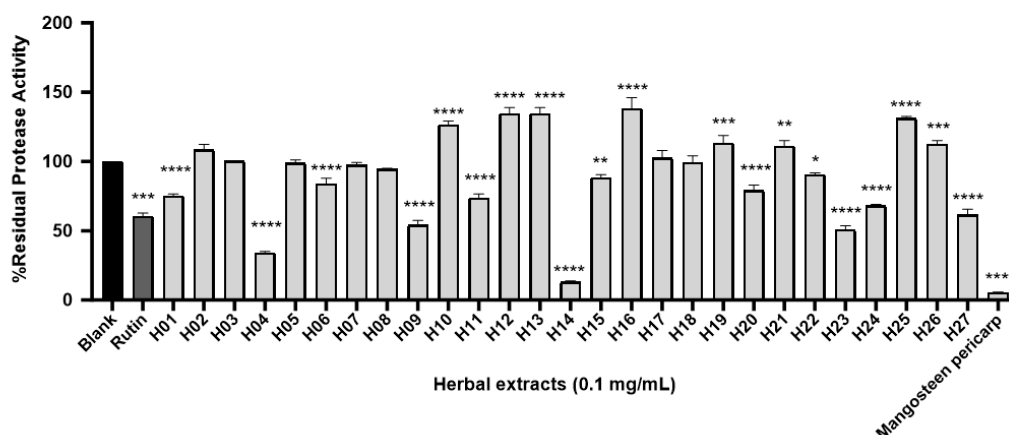


Figure 17. SARS-CoV-2 main protease (3CL^{Pro}) inhibition of herbal extracts (H01-H27 and mangosteen pericarp)

Each extract was tested at 0.1 mg/mL. The % residual protease activity of rutin and extracts were compared to that of blank compound without the inhibitor (negative control); * $p < 0.05$, ** $p < 0.001$, *** $p < 0.0001$ and **** $p < 0.00001$

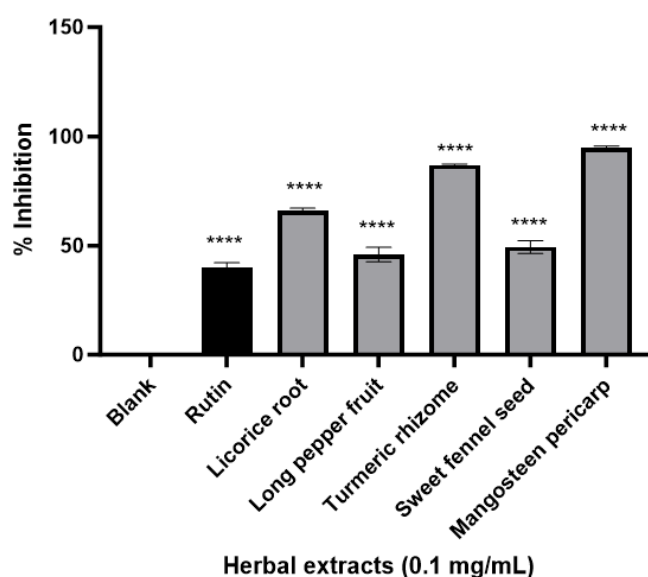


Figure 18. 3CL^{Pro} inhibitory activities of the most active herbal crude extracts at 0.1 mg/mL

Licorice root, long pepper fruit, turmeric rhizome, sweet fennel seed and mangosteen fruit pericarp showed $66.1\% \pm 1.1$, $45.8\% \pm 3.3$, $86.9\% \pm 0.5$, $49.3\% \pm 3.0$ and $94.9\% \pm 0.64$ inhibition respectively. Rutin (positive control) was tested at 100 μ M. The relative 3CL^{Pro} inhibition of rutin at 100 μ M was $39.7\% \pm 2.4$. The % inhibition of rutin and extracts were compared to that of blank compound without the inhibitor (negative control); **** $p < 0.00001$

4.1.1. Discussion

From this study, some of the herbal extracts such as mangosteen, turmeric, licorice, sweet fennel and long pepper showed promising *in vitro* 3CL^{Pro} inhibitory activity. Our findings corresponded with the study done by Bahun et al. in which curcumin, an active compound from turmeric rhizome, exhibited substantial 3CL^{Pro} inhibitory activity against SARS-CoV-2 virus [6]. In addition, Guijarro-Real et al. described that turmeric extract significantly inhibited 3CL^{Pro} activity (5). Moreover, van de Sand et al. demonstrated that glycyrrhizin, a major phytochemical from licorice root has potent *in vitro* 3CL^{Pro} inhibitory effect (7). Furthermore, Wansri et al. reported the *in vitro* anti-SARS-CoV-2 3CL^{Pro} activity of piperine, which is one of the active phytochemicals in both black pepper and long pepper fruits (8). The 3CL^{Pro} inhibitory activity by sweet fennel seeds, however, has been explained for the first time in this study. Last but not least, the mangosteen pericarp extract showed the most promising *in vitro* 3CL^{Pro} inhibitory activity. According to Ovalle-Magallanes et al. and Kurose et al., the alpha-mangostin compound is mostly studied due to its highest percentage yield of 78% by weight among all the natural xanthones from the dry mangosteen pericarp extract (11, 30). Also, the potential SARS-CoV-2 main protease inhibitory activity of alpha-mangostin has been investigated recently (8, 17, 18). Hence, alpha-mangostin has been selected as the interested bioactive compound in this study to further evaluate its potential SARS-CoV-2 main protease inhibitory activity.

However, alpha-mangostin has hydrophobic nature which limits its biological activities and therapeutic efficacy. Therefore, alpha-mangostin loaded nanocarriers have been designed to overcome this limitation, and polymeric micelles are the

promising nanocarriers for hydrophobic alpha-mangostin compound due to the presence of a robust core-shell structure of polymeric micelles and their intrinsic ability to improve the solubility of alpha-mangostin, thereby enhancing its bioavailability.

4.2. Preparation of alpha-mangostin loaded polymeric micelles with Soluplus[®] concentration of 1 mg/mL

First of all, different concentrations of alpha-mangostin loaded polymeric micelles such as 2.5% w/w, 5% w/w and 10% w/w formulations were prepared with Soluplus[®] at the concentration of 1 mg/mL by using a thin-film hydration method.

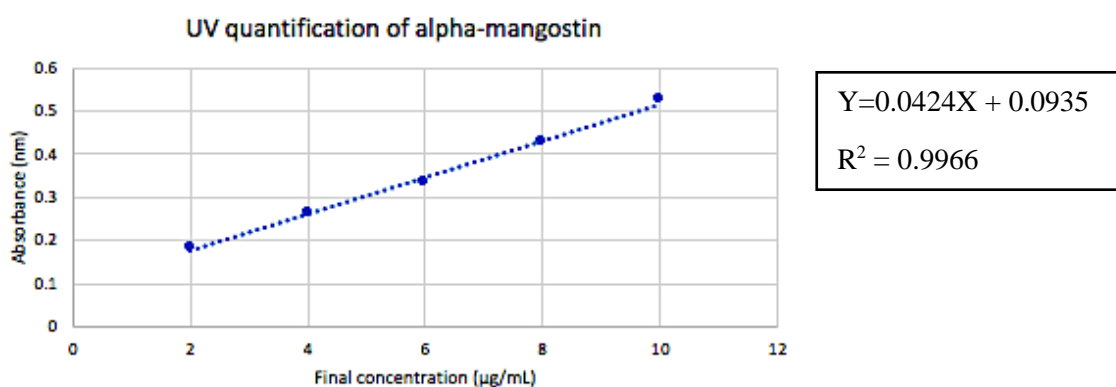
4.2.1. Preliminary analyses of encapsulation efficiency (%EE) and loading capacity (%LC) of alpha-mangostin loaded polymeric micelles with UV-vis spectrophotometer

The preliminary analyses of encapsulation efficiency (%EE) and loading capacity (%LC) of 2.5% w/w, 5% w/w and 10% w/w alpha-mangostin loaded polymeric micelles at Soluplus[®] concentration of 1 mg/mL were undertaken with UV-vis spectrophotometer. The UV quantitative analysis of alpha-mangostin content, and the preparation of standard calibration curve (average of 3 replicates) were based on the protocol from a previous study (44) with slight modifications (**Table 3.** and **Figure 19**).

Table 3. Analysis of alpha-mangostin content with UV-vis spectrophotometer

- Final concentration range: 2µg/mL - 10µg/mL
- UV wavelength: 320nm

Final concentration (µg/mL)	Absorbance (nm)
2	0.184
4	0.264
6	0.336
8	0.429
10	0.525

**Figure 19.** Standard calibration curve for quantification of alpha-mangostin with UV

The UV absorbance values of 2.5% w/w and 5% w/w alpha-mangostin loaded polymeric micelles formulations were within the standard calibration curve range whereas the UV absorbance values of 10% w/w alpha-mangostin loaded polymeric micelles formulation were outside of the standard calibration curve range. Hence, the encapsulation efficiency (%EE) and loading capacity (%LC) of 2.5% w/w and 5% w/w formulations were only analysed with UV.

The preliminary UV analysis results of encapsulation efficiency (%EE) and loading capacity (%LC) of 2.5% w/w and 5% w/w alpha-mangostin loading polymeric micelles formulations were presented in **Table 4**.

Table 4. Preliminary analyses of %EE and %LC with UV-vis spectrophotometer

%EE and %LC	2.5% w/w	5% w/w
Encapsulation Efficiency% (%EE)	60.61% ± 2.15	86.51% ± 1.06
Loading Capacity% (%LC)	1.48% ± 0.05	4.12% ± 0.05

2.5% w/w formulation was made up of 0.025 mg/mL alpha-mangostin and 1mg/mL Soluplus®

5% w/w formulation was made up of 0.05 mg/mL alpha-mangostin and 1mg/mL Soluplus®

The results were presented as mean ± standard deviation of three independent experiments

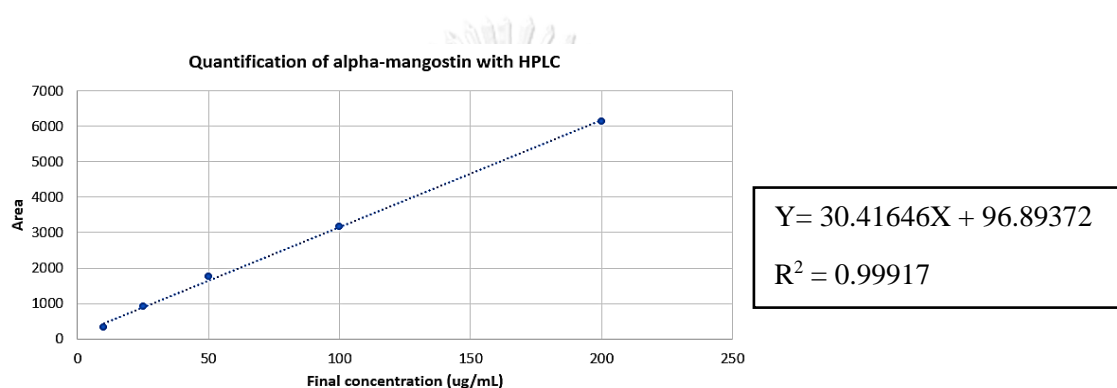
4.2.2. Preliminary analyses of encapsulation efficiency (%EE) and loading capacity (%LC) of alpha-mangostin loaded polymeric micelles with HPLC

The preliminary analyses of encapsulation efficiency (%EE) and loading capacity (%LC) of 2.5% w/w, 5% w/w and 10% w/w alpha-mangostin loaded polymeric micelles at Soluplus® concentration of 1 mg/mL were undertaken with HPLC technique. The HPLC quantitative analysis of alpha-mangostin content, and the preparation of standard calibration curve (average of 3 replicates) were based on the protocol from a previous study (45) with slight modifications (**Table 5.** and **Figure 20**).

Table 5. Analysis of alpha-mangostin content with HPLC

- Final concentration range: 10 μ g/mL - 200 μ g/mL
- UV wavelength: 320nm

Final concentration (μ g/mL)	Area
10	322.10783
25	922.94250
50	1762.08097
100	3154.72080
200	6131.84619

**Figure 20.** Standard calibration curve for quantification of alpha-mangostin with HPLC

The results of 2.5% w/w and 10% w/w alpha-mangostin loaded polymeric micelles formulations did not show any peak within HPLC standard calibration curve range. Only the results of 5% w/w alpha-mangostin loaded polymeric micelles formulation showed peak within HPLC standard calibration curve range. Hence, the encapsulation efficiency (%EE) and loading capacity (%LC) of 5% w/w formulation was only analysed with HPLC.

The preliminary HPLC analysis results of encapsulation efficiency (%EE) and loading capacity (%LC) of 5% w/w alpha-mangostin loading polymeric micelles formulation at Soluplus[®] concentration of 1 mg/mL were presented in **Table 6**.

Table 6. Preliminary HPLC analyses of %EE and %LC of 5% w/w alpha-mangostin loaded polymeric micelles formulation at Soluplus® concentration of 1 mg/mL

%EE and %LC	5% w/w
Encapsulation Efficiency% (%EE)	86.07% ± 3.25
Loading Capacity% (%LC)	4.10% ± 0.16

5% w/w formulation was made up of 0.05 mg/mL alpha-mangostin and 1mg/mL Soluplus®

The results were presented as mean ± standard deviation of three independent experiments

4.2.3. Preliminary characterizations of alpha-mangostin loaded polymeric micelles

The preliminary characterizations in terms of hydrodynamic diameter, polydispersity index (PDI) and zeta potential of alpha-mangostin loaded polymeric micelles of 2.5% w/w, 5% w/w and 10% w/w formulations were presented in **Table 7.**

Table 7. Preliminary characterizations of alpha-mangostin loaded polymeric micelles

Characterizations	2.5% w/w	5% w/w	10% w/w
Size (Mean Z-average) (nm)	44.36 ± 0.36	58.16 ± 0.25	70.59 ± 0.95
Polydispersity index	0.0703 ± 0.0050	0.1262 ± 0.0090	0.1646 ± 0.0200
Zeta Potential (mV)	-16.54 ± 2.74	-17.00 ± 2.49	-14.99 ± 2.04

2.5% w/w formulation was made up of 0.025 mg/mL alpha-mangostin and 1mg/mL Soluplus®

5% w/w formulation was made up of 0.05 mg/mL alpha-mangostin and 1mg/mL Soluplus®

10% w/w formulation was made up of 0.1 mg/mL alpha-mangostin and 1mg/mL Soluplus®

The results were presented as mean ± standard deviation of three independent experiments

4.2.4. Discussion

The UV absorbance values of 2.5% w/w and 5% w/w alpha-mangostin loaded polymeric micelles formulations were within the standard calibration curve range whereas the UV absorbance values of 10% w/w alpha-mangostin loaded polymeric micelles formulation were outside of the standard calibration curve range. Therefore, the 10% w/w alpha-mangostin loaded polymeric micelles formulation was ruled out for the evaluation of % encapsulation efficiency and % loading capacity by UV. Based on the preliminary UV analyses, the 2.5% w/w alpha-mangostin loaded polymeric micelles formulation had an encapsulation efficiency of $60.61\% \pm 2.15$, and a loading capacity of $1.48\% \pm 0.05$. Meanwhile, the 5% w/w alpha-mangostin loaded polymeric micelles formulation had an encapsulation efficiency of $86.51\% \pm 1.06$, and a loading capacity of $4.12\% \pm 0.05$.

Regarding the preliminary HPLC analyses of alpha-mangostin loaded polymeric micelles, the results of 2.5% w/w and 10% w/w alpha-mangostin loaded polymeric micelles formulations did not show any peak within the HPLC standard calibration curve range. Only the results of 5% w/w alpha-mangostin loaded polymeric micelles formulation showed the peak within HPLC standard calibration curve range. The 5% w/w alpha-mangostin loaded polymeric micelles formulation from HPLC analysis showed an encapsulation efficiency of $86.07\% \pm 3.25$, and a loading capacity of $4.10\% \pm 0.156$, which were similar to the results from UV analyses of 5% w/w alpha-mangostin loaded polymeric micelles formulation.

The results of preliminary characterization in terms of polydispersity index (PDI) and zeta-potential of alpha-mangostin loaded polymeric micelles of 2.5% w/w, 5% w/w and 10% w/w formulations were not significant although an increasing trend

in hydrodynamic diameters were observed when the formulation ratio was increased from 2.5% w/w, to 5% w/w and 10% w/w.

Based on the preliminary results, 5% w/w alpha-mangostin loaded polymeric micelles seemed to be the most promising formulation due to its high encapsulation efficiency and loading capacity. Hence, the 5% w/w formulation was selected to investigate further with higher Soluplus[®] concentrations and higher alpha-mangostin concentrations for higher encapsulation efficiency, loading capacity and the other characterization parameters.

4.3. Preparation of 5% w/w alpha-mangostin loaded polymeric micelles with Soluplus[®] concentration of 2 mg/mL

The 5% w/w alpha-mangostin loaded polymeric micelles were prepared with Soluplus[®] at the concentration of 2 mg/mL and alpha-mangostin concentration of 0.1 mg/mL.

4.3.1. HPLC analyses of encapsulation efficiency (%EE) and loading capacity (%LC) of 5%w/w alpha-mangostin loaded polymeric micelles with Soluplus[®] concentration of 2 mg/mL

The HPLC analysis results of encapsulation efficiency (%EE) and loading capacity (%LC) of 5% w/w alpha-mangostin loading polymeric micelles formulation at Soluplus[®] concentration of 2 mg/mL were presented in **Table 8**.

Table 8. HPLC analyses of %EE and %LC of 5%w/w alpha-mangostin loaded polymeric micelles formulation at Soluplus® concentration of 2 mg/mL

%EE and %LC	5% w/w
Encapsulation Efficiency% (%EE)	90.23% ± 0.53
Loading Capacity% (%LC)	4.30% ± 0.03

5% w/w formulation was made up of 0.1 mg/mL alpha-mangostin and 2 mg/mL Soluplus®

The results were presented as mean ± standard deviation of three independent experiments

4.3.2. Characterizations of 5%w/w alpha-mangostin loaded polymeric micelles with Soluplus® concentration of 2 mg/mL

The characterizations in terms of hydrodynamic diameter, polydispersity index (PDI) and zeta-potential of alpha-mangostin loaded polymeric micelles of 5% w/w formulation with Soluplus® concentration of 2 mg/mL were presented in **Table 9**.

Table 9. Characterizations of 5% w/w alpha-mangostin loaded polymeric micelles with Soluplus® concentration of 2 mg/mL

Characterizations	5% w/w
Size (Mean Z-average) (nm)	69.18 ± 1.05
Polydispersity index	0.1190 ± 0.0200
Zeta Potential (mV)	-16.47 ± 0.37

5% w/w formulation was made up of 0.1 mg/mL alpha-mangostin and 2 mg/mL Soluplus®

The results were presented as mean ± standard deviation of three independent experiments

4.4. Preparation of 5% w/w alpha-mangostin loaded polymeric micelles with Soluplus[®] concentration of 4 mg/mL

The 5% w/w alpha-mangostin loaded polymeric micelles were prepared with Soluplus[®] at the concentration of 4 mg/mL and alpha-mangostin concentration of 0.2 mg/mL.

4.4.1. HPLC analyses of encapsulation efficiency (%EE) and loading capacity (%LC) of 5%w/w alpha-mangostin loaded polymeric micelles with Soluplus[®] concentration of 4 mg/mL

The HPLC analysis results of encapsulation efficiency (%EE) and loading capacity (%LC) of 5% w/w alpha-mangostin loading polymeric micelles formulation at Soluplus[®] concentration of 4 mg/mL were presented in **Table 10**.

Table 10. HPLC analyses of %EE and %LC of 5%w/w alpha-mangostin loaded polymeric micelles formulation at Soluplus[®] concentration of 4 mg/mL

%EE and %LC	5% w/w
Encapsulation Efficiency% (%EE)	91.65% ± 0.27
Loading Capacity% (%LC)	4.36% ± 0.01

5% w/w formulation was made up of 0.2 mg/mL alpha-mangostin and 4 mg/mL Soluplus[®]

The results were presented as mean ± standard deviation of three independent experiments

4.4.2. Characterizations of 5%w/w alpha-mangostin loaded polymeric micelles with Soluplus[®] concentration of 4 mg/mL

The characterizations in terms of hydrodynamic diameter, polydispersity index (PDI) and zeta-potential of alpha-mangostin loaded polymeric micelles of 5% w/w formulation with Soluplus[®] concentration of 4 mg/mL were presented in **Table 11**.

Table 11. Characterizations of 5% w/w alpha-mangostin loaded polymeric micelles with Soluplus[®] concentration of 4 mg/mL

Characterizations	5% w/w
Size (Mean Z-average) (nm)	73.00 ± 3.48
Polydispersity index	0.1490 ± 0.0010
Zeta Potential (mV)	-16.54 ± 0.67

5% w/w formulation was made up of 0.2 mg/mL alpha-mangostin and 4 mg/mL Soluplus[®]

The results were presented as mean ± standard deviation of three independent experiments

4.5. Preparation of 5% w/w alpha-mangostin loaded polymeric micelles with Soluplus[®] concentration of 10 mg/mL

The 5% w/w alpha-mangostin loaded polymeric micelles were prepared with Soluplus[®] at the concentration of 10 mg/mL and alpha-mangostin concentration of 0.5 mg/mL.

4.5.1. HPLC analyses of encapsulation efficiency (%EE) and loading capacity (%LC) of 5%w/w alpha-mangostin loaded polymeric micelles with Soluplus® concentration of 10 mg/mL

The HPLC analysis results of encapsulation efficiency (%EE) and loading capacity (%LC) of 5% w/w alpha-mangostin loading polymeric micelles formulation at Soluplus® concentration of 10 mg/mL were presented in **Table 12**.

Table 12. HPLC analyses of %EE and %LC of 5%w/w alpha-mangostin loaded polymeric micelles formulation at Soluplus® concentration of 10 mg/mL

%EE and %LC	5% w/w
Encapsulation Efficiency% (%EE)	95.65% ± 0.21
Loading Capacity% (%LC)	4.56% ± 0.01

5% w/w formulation was made up of 0.5 mg/mL alpha-mangostin and 10 mg/mL Soluplus®

The results were presented as mean ± standard deviation of three independent experiments

4.5.2. Characterizations of 5%w/w alpha-mangostin loaded polymeric micelles with Soluplus® concentration of 10 mg/mL

The characterizations in terms of hydrodynamic diameter, polydispersity index (PDI) and zeta-potential of alpha-mangostin loaded polymeric micelles of 5% w/w formulation with Soluplus® concentration of 10 mg/mL were presented in **Table 13**.

Table 13. Characterizations of 5% w/w alpha-mangostin loaded polymeric micelles with Soluplus[®] concentration of 10 mg/mL

Characterizations	5% w/w
Size (Mean Z-average) (nm)	97.43 ± 0.48
Polydispersity index	0.1680 ± 0.0090
Zeta Potential (mV)	-18.02 ± 0.28

5% w/w formulation was made up of 0.5 mg/mL alpha-mangostin and 10 mg/mL Soluplus[®]

The results were presented as mean ± standard deviation of three independent experiments.

4.6. Discussion

Since 5% w/w alpha-mangostin loaded polymeric micelles seemed to be the most promising formulation in terms of its high encapsulation efficiency, loading capacity and acceptable range of characterizations, it was selected as an interested formulation for further investigations in this study. Higher Soluplus[®] concentrations and higher alpha-mangostin concentrations were used to find out for higher encapsulation efficiency, loading capacity and the other characterization parameters. The results of encapsulation efficiency (%EE), loading capacity (%LC) and characterizations of 5% w/w alpha-mangostin loaded polymeric micelles formulations with different concentrations of Soluplus[®] and alpha-mangostin were presented in **Table 14**.

Table 14. Summary of % EE, %LC and Characterizations of 5%w/w formulations

Evaluation Parameters	5%w/w [Soluplus]=1mg/mL [AM]=0.05mg/mL	5%w/w [Soluplus]=2mg/mL [AM]=0.1mg/mL	5%w/w [Soluplus]=4mg/mL [AM]=0.2mg/mL	5%w/w [Soluplus]=10mg/mL [AM]=0.5mg/mL
Encapsulation Efficiency %	86.07% ± 3.25	90.23% ± 0.53	91.65% ± 0.27	95.65% ± 0.21
Loading Capacity %	4.10% ± 0.16	4.30% ± 0.03	4.36% ± 0.01	4.56% ± 0.01
Hydrodynamic diameter/Size (nm)	58.16 ± 0.25	69.18 ± 1.05	73.00 ± 3.48	97.43 ± 0.48
Polydispersity Index (PDI)	0.1262 ± 0.0090	0.1190 ± 0.0200	0.1490 ± 0.0010	0.1680 ± 0.0090
Zeta potential (mV)	-17.00 ± 2.49	-16.47 ± 0.37	-16.54 ± 0.67	-18.02 ± 0.28

It was evident that the encapsulation efficiency, loading capacity and hydrodynamic diameter increased as the concentrations of Soluplus[®] and alpha-mangostin were increased. When Soluplus[®] concentration was 1 mg/mL and alpha-mangostin concentration was 0.05 mg/mL, the encapsulation efficiency and loading capacity were 86.07% ± 3.25 and 4.10% ± 0.156 respectively. The hydrodynamic diameter was observed as 58.16 nm ± 0.25. The increasing trend in encapsulation efficiency, loading capacity and hydrodynamic diameter was investigated when Soluplus[®] concentration was increased to 2 mg/mL and alpha-mangostin was increased to 0.1 mg/mL. The encapsulation efficiency, loading capacity and hydrodynamic diameter were 90.23% ± 0.53, 4.30% ± 0.03, and 69.18 nm ± 1.05. When Soluplus[®] concentration and alpha-mangostin concentration were further increased to 4 mg/mL and 0.2 mg/mL, further increases in encapsulation efficiency of 91.65% ± 0.27, loading capacity of 4.36% ± 0.01 and hydrodynamic diameter of 73.00 nm ± 3.48 were observed. There were significant rises in encapsulation efficiency, loading capacity and hydrodynamic diameter when Soluplus[®]

concentration and alpha-mangostin concentration were used up to 10 mg/mL and 0.5 mg/mL respectively. The encapsulation efficiency of $95.65\% \pm 0.21$, loading capacity of $4.56\% \pm 0.01$, and hydrodynamic diameter of $97.43 \text{ nm} \pm 0.48$ were obtained. However, there was not any significant change in polydispersity index (PDI). The PDIs of all the formulations were less than 0.2. Regarding zeta-potential, there were not any significant changes. The zeta-potentials of all the formulations were between -16 mV and -18 mV. The presence of negative charge zeta potential of Soluplus[®] polymeric micelles was due to the interaction of polar functional group in Soluplus[®] with water molecules to form a hydrophilic shell (51). However, the fundamental behind the exact mechanism of the interactions involved has not been reported. Moreover, the small value of zeta-potential less than -20 mV was due to the higher availability of hydrophobic segments in promoting the formation of micelles with larger hydrophobic core (51). Although the zeta potential values larger than +30 mV and -30 mV are preferably recognized for high stability of micelles, the zeta potential values larger than +10 mV and -10 mV can still be considered for incipient stability of micelles (48). Nevertheless, the small particles size of less than 200 nm and the monodisperse distribution with the PDI of less than 0.3 are the important parameters of Soluplus[®] polymeric micelles to avoid the engulfment of alveolar macrophages, and to achieve the uniform drug absorption profile across the pulmonary mucosal barriers respectively if the intended formulation is for pulmonary route of administration (36). In addition, the negative surface charge of Soluplus[®] polymeric micelles as characterized by zeta-potential can facilitate the penetration of pulmonary mucus layer for paracellular transport or transcytosis mechanism (36).

Among all the 5% w/w alpha-mangostin loaded polymeric micelles formulations with different concentrations of Soluplus[®] and alpha-mangostin, it was evident that the formulation which was made up of 10 mg/mL Soluplus[®] and 0.5 mg/mL alpha-mangostin was the promising formulation in terms of highest encapsulation efficiency and loading capacity as well as its desirable characterizations results. Hence, the 5% w/w alpha-mangostin loaded polymeric micelles formulation with the concentrations of 10 mg/mL Soluplus[®] and 0.5 mg/mL alpha-mangostin was selected in this study for further investigations in morphology analysis and stability study as well as evaluations of SARS-CoV-2 main protease (3CL^{Pro}) inhibitory activity and *in vitro* cytotoxicity in HaCaT cells line.

4.7. Morphology analysis of 5%w/w alpha-mangostin loaded polymeric micelles with 10 mg/mL Soluplus[®] and 0.5 mg/mL alpha-mangostin

The morphology of both blank Soluplus[®] polymeric micelles and alpha-mangostin loaded Soluplus[®] polymeric micelles were observed by transmission electron microscopy (TEM) under negative staining with 2% uranyl acetate solution, which is one of the commonly used staining reagents to give a satisfactory contrast in TEM images (52). The TEM images of both blank Soluplus[®] polymeric micelles and alpha-mangostin loaded Soluplus[®] polymeric micelles were presented in **Figure 21** and **Figure 22**.

Red arrow (→) indicates polymeric micelles

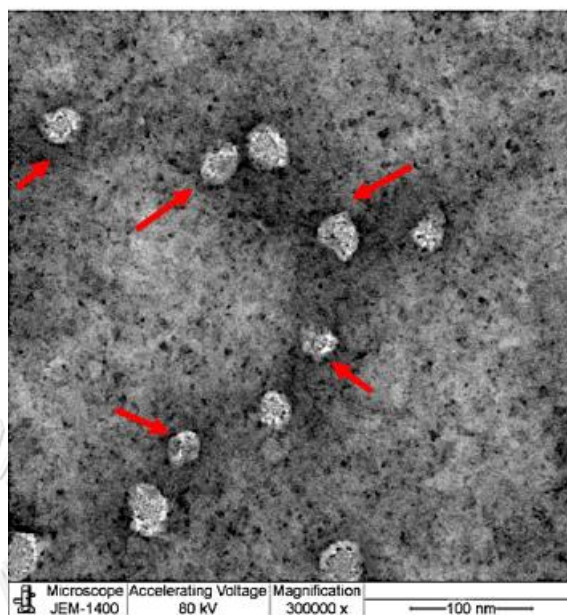


Figure 21. TEM image of blank Soluplus® polymeric micelles

Red arrow (→) indicates polymeric micelles

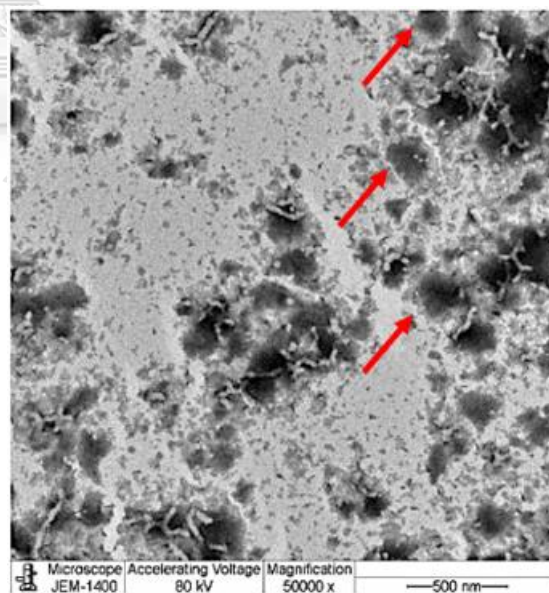


Figure 22. TEM image of 5% w/w alpha-mangostin loaded Soluplus® polymeric micelles

The physical appearances of both blank Soluplus[®] polymeric micelles and alpha-mangostin loaded Soluplus[®] polymeric micelles were presented in **Figure 23**.

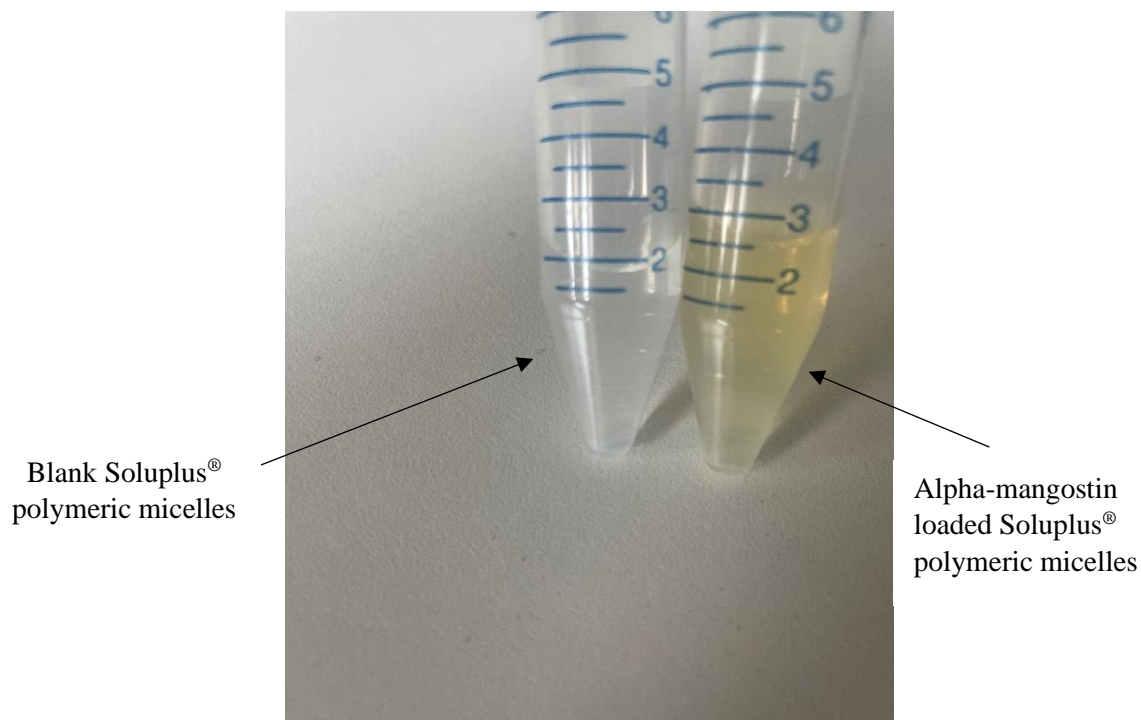


Figure 23. Physical appearances of blank Soluplus[®] polymeric micelles and alpha-mangostin loaded Soluplus[®] polymeric micelles

4.7.1. Discussion

Both blank Soluplus[®] polymeric micelles and alpha-mangostin loaded Soluplus[®] polymeric micelles showed spherical shape under TEM. An increase in hydrodynamic diameter of alpha-mangostin loaded Soluplus[®] polymeric micelles was noted as compared to the blank Soluplus[®] polymeric micelles. This was confirmed with the characterizations analysis by using a Zetasizer Pro (Malvern[™]). The

characterizations result of blank Soluplus[®] polymeric micelles and alpha-mangostin loaded Soluplus[®] polymeric micelles were presented in **Table 15**.

Table 15. Characterizations of blank Soluplus[®] polymeric micelles and alpha-mangostin loaded Soluplus[®] polymeric micelles

Characterizations	Blank made up of [Soluplus [®]] = 10 mg/mL	5% w/w made up of [Soluplus [®]] = 10 mg/mL [Alpha-mangostin] = 0.5 mg/mL
Hydrodynamic diameter/ Size (nm)	70.59 ± 0.95	97.43 ± 0.48
Polydispersity index (PDI)	0.1579 ± 0.0010	0.1680 ± 0.0090
Zeta potential (mV)	-17.33 ± 0.47	-18.02 ± 0.28

The results were presented as mean ± standard deviation of three independent experiments

The hydrodynamic diameter of alpha-mangostin loaded polymeric micelles was 97.43 nm ± 0.48, which was slightly larger than that of blank Soluplus[®] polymeric micelles (70.59 nm ± 0.95). However, there were not much significant changes in PDI and zeta-potential between the two formulations.

4.8. Stability study of 5%w/w alpha-mangostin loaded polymeric micelles with 10 mg/mL Soluplus[®] and 0.5 mg/mL alpha-mangostin

Alpha-mangostin loaded Soluplus[®] polymeric micelles of the selected formulation was kept at two different temperatures (4°C and 25°C) in the 15 mL conical tubes for 30 days. The changes in terms of encapsulation efficiency (%EE), loading capacity (%LC), hydrodynamic diameter, polydispersity index and zeta-potential were examined at 0, 1, 3, 5, 7, 14 and 30 days (**Table 16**).

Table 16. Stability study of 5% w/w alpha-mangostin loaded polymeric micelles

Room Temp (25 °C)	Day 0	Day 1	Day 3	Day 5	Day 7	Day 14	Day 30
Encapsulation Efficiency %	95.65% ± 0.21	95.61% ± 0.01	95.19% ± 0.04	95.16% ± 0.18	94.83% ± 0.12	91.38% ± 0.09	81.04% ± 0.15
Loading Capacity %	4.56% ± 0.01	4.55% ± 0.06	4.53% ± 0.01	4.53% ± 0.02	4.52% ± 0.01	4.35% ± 0.01	3.85% ± 0.01
Hydrodynamic diameter/Size (nm)	97.43 ± 0.48	97.10 ± 0.20	96.72 ± 0.28	96.38 ± 0.15	96.27 ± 0.17	91.43 ± 0.65	86.00 ± 0.66
Polydispersity index (PDI)	0.1680 ± 0.0090	0.1704 ± 0.0010	0.1725 ± 0.0010	0.1722 ± 0.0050	0.1676 ± 0.0030	0.1890 ± 0.0010	0.2047 ± 0.0060
Zeta potential (mV)	-18.02 ± 0.28	-17.27 ± 0.25	-17.81 ± 0.14	-17.61 ± 0.27	-17.67 ± 0.20	-16.04 ± 0.57	-13.41 ± 1.07

4°C	Day 0	Day 1	Day 3	Day 5	Day 7	Day 14	Day 30
Encapsulation Efficiency %	95.65% ± 0.21	95.56% ± 0.05	95.37% ± 0.14	95.25% ± 0.04	95.11% ± 0.18	95.00% ± 0.09	91.37% ± 0.03
Loading Capacity %	4.56% ± 0.01	4.55% ± 0.01	4.54% ± 0.01	4.54% ± 0.01	4.53% ± 0.01	4.52% ± 0.01	4.35% ± 0.01
Hydrodynamic diameter/Size (nm)	97.43 ± 0.48	97.33 ± 0.04	97.30 ± 0.17	97.22 ± 0.15	97.18 ± 0.10	92.96 ± 0.24	90.75 ± 0.40
Polydispersity index (PDI)	0.1680 ± 0.0090	0.1738 ± 0.0050	0.1747 ± 0.0090	0.1726 ± 0.0030	0.1714 ± 0.0100	0.1801 ± 0.0050	0.1946 ± 0.0050
Zeta potential (mV)	-18.02 ± 0.28	-17.35 ± 0.35	-17.57 ± 0.28	-17.55 ± 0.30	-17.68 ± 0.30	-17.12 ± 0.05	-16.25 ± 0.33

4.8.1. Discussion

In this study, only two different temperatures (4°C and 25°C) were selected for stability analysis instead of testing at high temperatures. This is to preliminarily investigate about the stability of formulation at room temperature which the experiments were performed. And 4°C was selected to investigate for better stability

at cooler temperature. A range of temperatures such as 70 °C, 40 °C, -20 °C will be selected for further stability studies in the future. From Day 0 to Day 5, there were not much significant changes in encapsulation efficiency, loading capacity, hydrodynamic diameter, polydispersity index and zeta-potential of the formulation kept at two different temperatures. However, there was a slight change in encapsulation efficiency of the formulation kept at room temperature on Day 7. There was a slight drop in encapsulation efficiency from $95.16\% \pm 0.18$ to $94.83\% \pm 0.12$. All the other parameters remained in the similar values. Meanwhile, the formulation kept at 4°C seemed to be still stable on Day 7. On Day 14, there was a further decrease in encapsulation efficiency of the formulation kept at room temperature to $91.38\% \pm 0.09$. The loading capacity was also decreased to $4.35\% \pm 0.01$. Moreover, the hydrodynamic diameter was decreased to $91.43 \text{ nm} \pm 0.65$. Furthermore, there were slight variations in polydispersity index and zeta-potential. On the other hand, there was not any significant difference in all the parameters of the formulation kept at 4°C. On Day 30, most of the parameters of the formulation kept at room temperature dropped considerably. The encapsulation efficiency and loading capacity were reduced to $81.04\% \pm 0.15$ and $3.85\% \pm 0.01$ respectively. The hydrodynamic diameter was decreased to $86.00 \text{ nm} \pm 0.66$, and the zeta-potential was reduced to $-13.41 \text{ mV} \pm 1.07$ while there was a slight change in polydispersity index. The formulation kept at 4°C started to deteriorate on Day 30. There were declines in encapsulation efficiency to $91.37\% \pm 0.03$, and loading capacity to $4.35\% \pm 0.00$. The hydrodynamic diameter was also decreased to $90.75 \text{ nm} \pm 0.400$ whereas there were only slight changes in polydispersity index and zeta-potential. Overall, the

formulation kept at 4°C seemed to be more stable as compared to the one kept at room temperature during the 30-day stability study period.

4.9. Comparative evaluations of SARS-CoV-2 main protease (3CL^{Pro}) inhibitory activity of alpha-mangostin without the nanocarrier and alpha-mangostin loaded in polymeric micelles

Alpha-mangostin compound dissolved in DMSO and alpha-mangostin loaded in Soluplus[®] polymeric micelles of the selected formulation were screened together to evaluate their inhibitory activity towards SARS-CoV-2 main protease (3CL^{Pro}). The analysis of inhibitory activity results was conducted with the initial rates of blank compound without the inhibitor and 100 nM PF-07321332 as a positive control. The % residual protease activity results were presented in **Figure 24**.

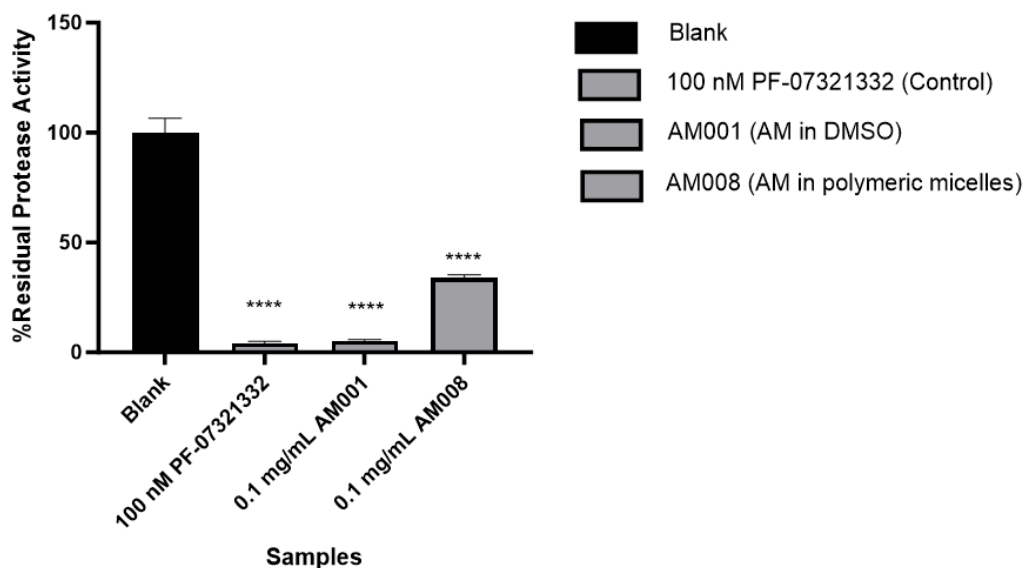


Figure 24. SARS-CoV-2 main protease (3CL^{Pro}) activity of samples. The % residual protease activity of control and samples were compared to that of blank compound without the inhibitor (negative control); ****p<0.00001

The % inhibitory activity results towards SARS-CoV-2 main protease (3CL^{Pro}) were presented in **Figure 25**.

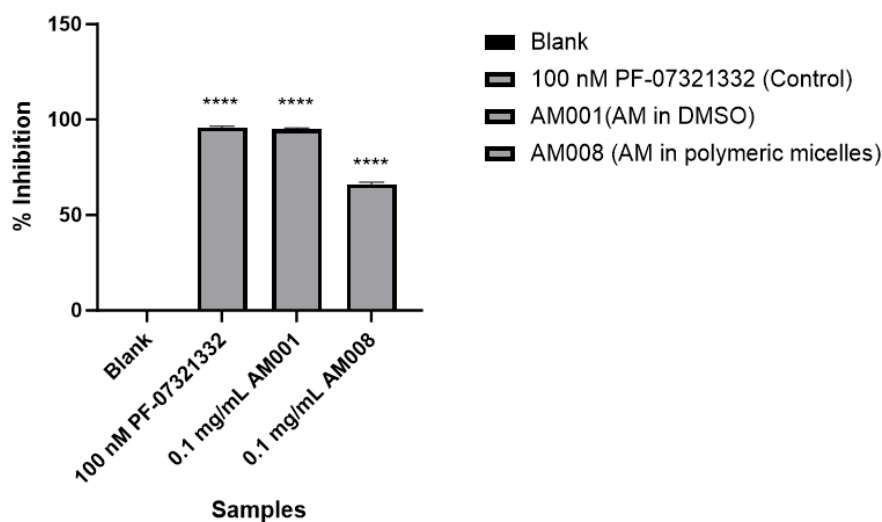


Figure 25. 3CL^{Pro} inhibitory activities of control and samples

The % inhibition of control and samples were compared to that of blank compound without the inhibitor (negative control); ****p<0.00001

4.9.1. Discussion

Both alpha-mangostin dissolved in DMSO (without the nanocarrier) and alpha-mangostin loaded in polymeric micelles showed significant inhibition of 3CL^{Pro} activity with residual protease activities of 5.15% ± 0.64, and 34.04% ± 1.30 respectively. The lower the residual % protease activity, the higher the inhibition of the 3CL^{Pro} activity of the samples. Alpha-mangostin dissolved in DMSO (AM001) showed 94.85% ± 0.64 inhibition, and alpha-mangostin loaded in polymeric micelles (AM008) showed 65.96% ± 1.30 inhibition respectively. PF-07321332 (positive control) was tested at 100 nM. The relative 3CL^{Pro} inhibition of control at 100 nM was 95.78% ± 0.77. The inhibitory activity towards 3CL^{Pro} was lower in alpha-

mangostin loaded polymeric micelles (65.96% inhibition; $IC_{50} = 140 \mu\text{g/mL}$) than that of alpha-mangostin dissolved in DMSO (94.85% inhibition; $IC_{50} = 26 \mu\text{g/mL}$). However, alpha-mangostin loaded polymeric micelles could still be considered as the promising formulation because its % inhibition towards 3CL^{Pro} was more than 50%. Moreover, the % 3CL^{Pro} inhibitory activity of alpha-mangostin loaded polymeric micelles was higher than that of rutin (positive control) which showed only $39.7\% \pm 2.4$ in the previous screening experiment.

4.10. Comparative *in vitro* cytotoxicity evaluations of alpha-mangostin without nanocarrier and alpha-mangostin loaded in polymeric micelles

Alpha-mangostin compound dissolved in DMSO (AM001) and alpha-mangostin loaded in Soluplus[®] polymeric micelles (AM008) of the selected 5% w/w formulation were evaluated for their *in vitro* cytotoxicity in HaCaT cells line by using 3-(4,5-dimethylthiazol-2-yl)-2,5-diphenyltetrazolium bromide (MTT) assay. The % cell viability results were presented in **Figure 26**.

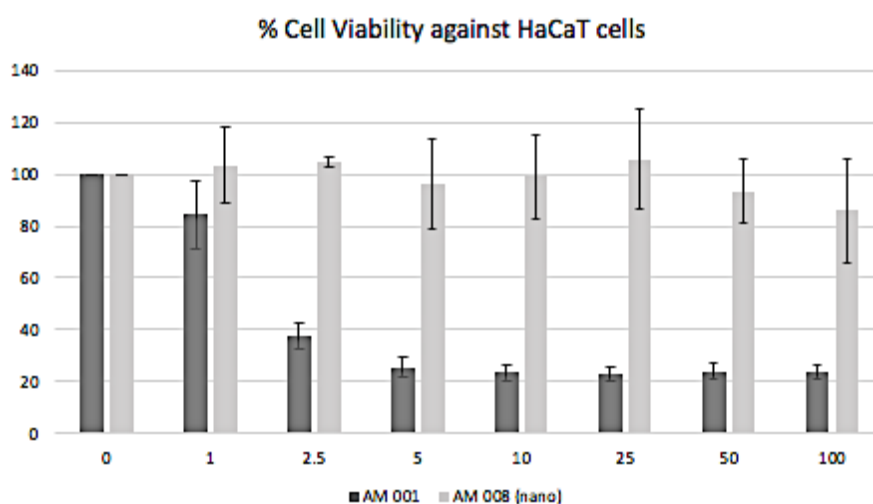


Figure 26. %Cell viability evaluation of alpha-mangostin dissolved in DMSO (AM001) and alpha-mangostin loaded in polymeric micelles (AM008) against HaCaT cells line

4.10.1. Discussion

HaCaT cells line (a spontaneously immortalized keratinocyte cells line from adult human skin) was used to evaluate *in vitro* cytotoxicity of alpha-mangostin without nanocarrier and alpha-mangostin loaded in polymeric micelles. The evaluation was performed on HaCaT cells line because it is one of the widely utilized cell models for investigation of cells viability (53). Although there are other types of cells line such as L929 or fibroblasts that can be used for cytotoxicity analysis, the immediate availability of HaCaT cells line in our laboratory facilitated the evaluation of cytotoxicity testing in a timely efficient way. Furthermore, the preliminary investigation of cytotoxicity testing on HaCaT cells line provided the general information about the toxicity of the compound and formulation towards normal cells before proceeding to the cytotoxicity testing with specific cells type for further studies in the future. It was observed that the % cell viability of 0.1mg/mL (100 µg/mL) of alpha-mangostin dissolved in DMSO (AM001) was 23.81%. Meanwhile, the % cell viability of 0.1mg/mL (100 µg/mL) of alpha-mangostin loaded in polymeric micelles (AM008) was 85.83%. According to these results, alpha-mangostin loaded in polymeric micelles showed lower cytotoxicity than alpha-mangostin compound. Hence, it can be noted that the toxicity of alpha-mangostin was reduced considerably when it was loaded in polymeric micelles.

CHAPTER 5. CONCLUSIONS

From this study, some of the selected herbal extracts such as turmeric rhizome, licorice root, sweet fennel seeds and long pepper fruits showed promising *in vitro* 3CL^{Pro} inhibitory activity. It was also evident that the pericarp extract of mangosteen fruit had the highest *in vitro* 3CL^{Pro} inhibitory activity. Among all the natural xanthenes from the dry mangosteen pericarp extract, alpha-mangostin compound is mostly studied due to its highest percentage yield by weight. Moreover, it has been investigated recently that the alpha-mangostin compound has potential SARS-CoV-2 main protease inhibitory activity. Hence, alpha-mangostin has been selected as the interested bioactive compound in this study to further evaluate its potential SARS-CoV-2 main protease inhibitory activity.

However, the hydrophobic nature of alpha-mangostin can affect its biological activities and therapeutic efficacy. In order to overcome this limitation, nanocarriers have been designed to encapsulate alpha-mangostin. Among all the nanocarriers, the polymeric micelles are the promising nanocarriers due to the presence of a robust core-shell structure to encapsulate the hydrophobic alpha-mangostin compound in the hydrophobic core of polymeric micelles, thereby improving the solubility and bioavailability of alpha-mangostin.

Three different concentrations of alpha-mangostin loaded polymeric micelles (2.5% w/w, 5% w/w and 10% w/w) formulations were prepared with Soluplus[®] at the concentration of 1 mg/mL by using a thin-film hydration method. Based on the preliminary results from UV and HPLC analyses, 5% w/w alpha-mangostin loaded polymeric micelles seemed to be the most promising formulation due to its high encapsulation efficiency and loading capacity. Hence, the 5% w/w formulation was

selected to investigate further with higher Soluplus[®] concentrations and higher alpha-mangostin concentrations for higher encapsulation efficiency, loading capacity and the other characterization parameters. Higher Soluplus[®] concentrations (2 mg/mL, 4 mg/mL, 10 mg/mL) and higher alpha-mangostin concentrations (0.1 mg/mL, 0.2 mg/mL, 0.5 mg/mL) were used respectively. It was evident that the encapsulation efficiency, loading capacity and hydrodynamic diameter increased as the concentrations of Soluplus[®] and alpha-mangostin were increased. However, there was not any significant changes in polydispersity index (PDI) and zeta-potential values.

Among all the 5% w/w alpha-mangostin loaded polymeric micelles formulations with different concentrations of Soluplus[®] and alpha-mangostin, it was investigated that the formulation which was made up of 10 mg/mL Soluplus[®] and 0.5 mg/mL alpha-mangostin was the promising formulation in terms of the highest encapsulation efficiency and loading capacity as well as the desirable characterizations results. In order to do further investigations in morphology analysis and stability study as well as evaluations of SARS-CoV-2 main protease (3CL^{Pro}) inhibitory activity and *in vitro* cytotoxicity in HaCaT cells line, the 5% w/w alpha-mangostin loaded polymeric micelles formulation with the concentrations of 10 mg/mL Soluplus[®] and 0.5 mg/mL alpha-mangostin was selected in this study.

The morphological analysis with TEM revealed that both blank Soluplus[®] polymeric micelles and alpha-mangostin loaded Soluplus[®] polymeric micelles had spherical shape. As compared to the blank Soluplus[®] polymeric micelles, an increase in hydrodynamic diameter of alpha-mangostin loaded Soluplus[®] polymeric micelles

was noted, which was also confirmed by using a Zetasizer Pro (Malvern™). Regarding the stability of the formulation, it was stable at both room temperature and 4°C for 5 days. However, the formulation kept at room temperature started to deteriorate steadily from Day 7 onwards. On the other hand, the formulation kept at 4°C remained stable until Day 14, and only started to deteriorate on Day 30. Overall, the formulation kept at 4°C seemed to be more stable as compared to the one kept at room temperature during the 30-day stability study period.

In order to evaluate their inhibitory activity towards SARS-CoV-2 main protease (3CL^{Pro}), alpha-mangostin compound dissolved in DMSO and alpha-mangostin loaded in Soluplus® polymeric micelles of the selected formulation were screened together. The % inhibition towards 3CL^{Pro} was lower in alpha-mangostin loaded polymeric micelles than that of alpha-mangostin dissolved in DMSO and the control. However, alpha-mangostin loaded polymeric micelles could still be considered as the promising formulation because its % inhibition towards 3CL^{Pro} was more than 50%. In addition, the comparative *in vitro* cytotoxicity evaluations of alpha-mangostin dissolved in DMSO and alpha-mangostin loaded in polymeric micelles showed that the % cell viability in HaCaT cells line was higher for alpha-mangostin loaded in polymeric micelles. According to these results, alpha-mangostin loaded in polymeric micelles displayed lower cytotoxicity than alpha-mangostin compound. Hence, it can be noted that the toxicity of alpha-mangostin was reduced considerably when it was loaded in polymeric micelles. Overall, alpha-mangostin can be loaded in Soluplus® polymeric micelles with high efficiency, and it showed the promising results towards SARS-CoV-2 main protease (3CL^{Pro}) inhibitory activity with lower cytotoxicity. These results will be useful for further studies.

REFERENCES

1. Lai C-C, Shih T-P, Ko W-C, Tang H-J, Hsueh P-R. Severe acute respiratory syndrome coronavirus 2 (SARS-CoV-2) and coronavirus disease-2019 (COVID-19): The epidemic and the challenges. *International journal of antimicrobial agents*. 2020;55(3):105924.
2. Kumar V, Alshazly H, Idris SA, Bourouis S. Evaluating the Impact of COVID-19 on Society, Environment, Economy, and Education. *Sustainability*. 2021;13(24):13642.
3. Charoensup R, Duangyod T, Phuneerub P, Pimpa R. Validation of Thai traditional medicine: Current scenario. Evidence-based validation of herbal medicine: Elsevier; 2022. p. 691-701.
4. Zhang L, Lin D, Sun X, Curth U, Drosten C, Sauerhering L, et al. Crystal structure of SARS-CoV-2 main protease provides a basis for design of improved α -ketoamide inhibitors. *Science*. 2020;368(6489):409-12.
5. Guijarro-Real C, Plazas M, Rodríguez-Burruezo A, Prohens J, Fita A. Potential in vitro inhibition of selected plant extracts against SARS-CoV-2 chymotrypsin-like protease (3CLPro) activity. *Foods*. 2021;10(7):1503.
6. Bahun M, Jukić M, Oblak D, Kranjc L, Bajc G, Butala M, et al. Inhibition of the SARS-CoV-2 3CLpro main protease by plant polyphenols. *Food chemistry*. 2022;373:131594.
7. van de Sand L, Bormann M, Alt M, Schipper L, Heilingloh CS, Steinmann E, et al. Glycyrrhizin effectively inhibits SARS-CoV-2 replication by inhibiting the viral main protease. *Viruses*. 2021;13(4):609.
8. Wansri R, Lin ACK, Pengon J, Kamchonwongpaisan S, Srimongkolpithak N, Rattanajak R, et al. Semi-synthesis of N-aryl amide analogs of piperine from *Piper nigrum* and evaluation of their antitrypanosomal, antimalarial, and anti-SARS-CoV-2 main protease activities. *Molecules*. 2022;27(9):2841.
9. Pyae NYL, Maiuthed A, Phongsopitanun W, Ouengwanarat B, Sukma W, Srimongkolpithak N, et al. N-Containing α -Mangostin Analogs via Smiles Rearrangement as the Promising Cytotoxic, Antitrypanosomal, and SARS-CoV-2 Main Protease Inhibitory Agents. *Molecules*. 2023;28(3):1104.
10. Do HTT, Cho J. Mangosteen pericarp and its bioactive xanthenes: Potential therapeutic value in Alzheimer's disease, Parkinson's disease, and depression with pharmacokinetic and safety profiles. *International journal of molecular sciences*. 2020;21(17):6211.
11. Ovalle-Magallanes B, Eugenio-Pérez D, Pedraza-Chaverri J. Medicinal properties of mangosteen (*Garcinia mangostana* L.): A comprehensive update. *Food and Chemical Toxicology*. 2017;109:102-22.
12. Pérez-Rojas JM, Cruz C, García-López P, Sánchez-González DJ, Martínez-Martínez CM, Ceballos G, et al. Renoprotection by α -mangostin is related to the attenuation in renal oxidative/nitrosative stress induced by cisplatin nephrotoxicity. *Free radical research*. 2009;43(11):1122-32.
13. Hung S-H, Shen K-H, Wu C-H, Liu C-L, Shih Y-W. α -Mangostin suppresses PC-3 human prostate carcinoma cell metastasis by inhibiting matrix metalloproteinase-2/9 and urokinase-plasminogen expression through the JNK signaling pathway. *Journal of agricultural and food chemistry*. 2009;57(4):1291-8.

14. Chen L-G, Yang L-L, Wang C-C. Anti-inflammatory activity of mangostins from *Garcinia mangostana*. *Food and Chemical Toxicology*. 2008;46(2):688-93.
15. Suksamrarn S, Suwannapoch N, Phakhodee W, Thanuhiranlert J, Ratananukul P, Chimnoi N, et al. Antimycobacterial activity of prenylated xanthenes from the fruits of *Garcinia mangostana*. *Chemical and pharmaceutical bulletin*. 2003;51(7):857-9.
16. Tarasuk M, Songprakhon P, Chieochansin T, Choomee K, Na-Bangchang K, Yenchitsomanus P-t. Alpha-mangostin inhibits viral replication and suppresses nuclear factor kappa B (NF- κ B)-mediated inflammation in dengue virus infection. *Scientific Reports*. 2022;12(1):16088.
17. Eleftheriou P, Amanatidou D, Petrou A, Geronikaki A. In silico evaluation of the effectivity of approved protease inhibitors against the main protease of the novel SARS-CoV-2 virus. *Molecules*. 2020;25(11):2529.
18. Hidayat S, Ibrahim FM, Pratama KF, Muchtaridi M. The interaction of alpha-mangostin and its derivatives against main protease enzyme in COVID-19 using in silico methods. *Journal of Advanced Pharmaceutical Technology & Research*. 2021;12(3):285.
19. Aisha AF, Ismail Z, Abu-Salah KM, Majid AMSA. Solid dispersions of α -mangostin improve its aqueous solubility through self-assembly of nanomicelles. *Journal of Pharmaceutical Sciences*. 2012;101(2):815-25.
20. Shi N-Q, Lai H-W, Zhang Y, Feng B, Xiao X, Zhang H-M, et al. On the inherent properties of Soluplus and its application in ibuprofen solid dispersions generated by microwave-quench cooling technology. *Pharmaceutical Development and Technology*. 2018;23(6):573-86.
21. Mohapatra D, Kumar DN, Shreya S, Pandey V, Dubey PK, Agrawal AK, et al. Quality by design-based development and optimization of fourth-generation ternary solid dispersion of standardized Piper longum extract for melanoma therapy. *Drug Delivery and Translational Research*. 2023:1-38.
22. Fang J, Chen Z, Song J, Li J, Han Y, Hou W, et al. Biodegradable self-assembly micelles significantly enhanced the solubility, biological stability and in vivo antitumor efficacy of Hexylselen. *RSC Chemical Biology*. 2021;2(6):1669-81.
23. Pignatello R, Corsaro R, Bonaccorso A, Zingale E, Carbone C, Musumeci T. Soluplus® polymeric nanomicelles improve solubility of BCS-class II drugs. *Drug Delivery and Translational Research*. 2022;12(8):1991-2006.
24. Sofroniou C, Baglioni M, Mamusa M, Resta C, Douth J, Smets J, et al. Self-Assembly of Soluplus in Aqueous Solutions: Characterization and Prospectives on Perfume Encapsulation. *ACS applied materials & interfaces*. 2022;14(12):14791-804.
25. Alopaeus JF, Hagesæther E, Tho I. Micellisation mechanism and behaviour of Soluplus®-furosemide micelles: Preformulation studies of an oral nanocarrier-based system. *Pharmaceuticals*. 2019;12(1):15.
26. Cui W, Yang K, Yang H. Recent progress in the drug development targeting SARS-CoV-2 main protease as treatment for COVID-19. *Frontiers in molecular biosciences*. 2020;7:616341.
27. Paxlovid™ (Nirmatrelvir tablets; Ritonavir tablets) For Patients 2023 [Available from: <https://www.paxlovid.com/>].
28. Marzi M, Vakil MK, Bahmanyar M, Zarenezhad E. Paxlovid: mechanism of action, synthesis, and in silico study. *BioMed Research International*. 2022;2022.
29. Rahman F, Tabrez S, Ali R, Alqahtani AS, Ahmed MZ, Rub A. Molecular

docking analysis of rutin reveals possible inhibition of SARS-CoV-2 vital proteins. *Journal of traditional and complementary medicine*. 2021;11(2):173-9.

30. Kurose H, Shibata M-A, Iinuma M, Otsuki Y. Alterations in cell cycle and induction of apoptotic cell death in breast cancer cells treated with α -mangostin extracted from mangosteen pericarp. *BioMed Research International*. 2012;2012.

31. Vats SK, Gupta RN, Ramaraju K, Singh R. Design and Statistical Evaluation of A Multiunit Delivery System Containing Nisoldipine-Soluplus® Solid Dispersion For Hypertension Chronotherapy. *International Journal of Pharmacy and Pharmaceutical Sciences* 2016;8:1-8.

32. Jin IS, Jo MJ, Park C-W, Chung YB, Kim J-S, Shin DH. Physicochemical, pharmacokinetic, and toxicity evaluation of soluplus® polymeric micelles encapsulating fenbendazole. *Pharmaceutics*. 2020;12(10):1000.

33. Varela-Garcia A, Concheiro A, Alvarez-Lorenzo C. Soluplus micelles for acyclovir ocular delivery: Formulation and cornea and sclera permeability. *International Journal of Pharmaceutics*. 2018;552(1-2):39-47.

34. Grotz E, Tateosian NL, Salgueiro J, Bernabeu E, Gonzalez L, Manca ML, et al. Pulmonary delivery of rifampicin-loaded soluplus micelles against *Mycobacterium tuberculosis*. *Journal of Drug Delivery Science and Technology*. 2019;53:101170.

35. Dian L, Yu E, Chen X, Wen X, Zhang Z, Qin L, et al. Enhancing oral bioavailability of quercetin using novel soluplus polymeric micelles. *Nanoscale research letters*. 2014;9:1-11.

36. Sipos B, Bella Z, Gróf I, Veszélka S, Deli MA, Szűcs KF, et al. Soluplus® promotes efficient transport of meloxicam to the central nervous system via nasal administration. *International Journal of Pharmaceutics*. 2023;632:122594.

37. BASF. Technical Information. Soluplus For better solubility and bioavailability. 2023 [Available from: <https://pharma.basf.com/files/one-page-promotions/soluplus-better-solubility-bioavailability-wet-granulation.pdf>]

38. BASF. Trade News. BASF Pharma Solutions excipient accepted into FDA Pilot Program for novel excipients 2022 [Available from: <https://basf.com/global/en/media/news-releases/2022/12/p-22-416>].

39. Rani S, Mishra S, Sharma M, Nandy A, Mozumdar S. Solubility and stability enhancement of curcumin in Soluplus® polymeric micelles: a spectroscopic study. *Journal of Dispersion Science and Technology*. 2020;41(4):523-36.

40. Yang H, Teng F, Wang P, Tian B, Lin X, Hu X, et al. Investigation of a nanosuspension stabilized by Soluplus® to improve bioavailability. *International journal of pharmaceutics*. 2014;477(1-2):88-95.

41. Kamaly N, Yameen B, Wu J, Farokhzad OC. Degradable controlled-release polymers and polymeric nanoparticles: mechanisms of controlling drug release. *Chemical reviews*. 2016;116(4):2602-63.

42. Committee TP. Thai Herbal Pharmacopoeia 2021 Bureau of Drug and Narcotic, Department of Medical Sciences, Ministry of Public Health 2021 [Available from: <https://bdn.go.th/thp/home>].

43. Pooma R SS. Plant Names of Thailand. Tem Smitinand's Thai Plant Names, Forest Herbarium BKF. Department of National Park, Bangkok 2014.

44. Pothitirat W, Gritsanapan W. Quantitative analysis of total mangostins in *Garcinia mangostana* fruit rind. *J Health Res*. 2008;22(4):161-6.

45. Pothitirat W, Gritsanapan W. HPLC quantitative analysis method for the

determination of α -mangostin in mangosteen fruit rind extract. Thai Journal of Agricultural Science. 2009;42(1):7-12.

46. Maguire CM, Rösslein M, Wick P, Prina-Mello A. Characterisation of particles in solution—a perspective on light scattering and comparative technologies. Science and technology of advanced materials. 2018;19(1):732-45.

47. Kushwaha K, Mishra MK, Srivastava R. Fabrication and Characterization of Pluronic F68 and Phospholipon 90g Embedded Nanoformulation for Sertraline Delivery: An Optimized Factorial Design Approach and In Vivo Study. Asian Journal of Pharmaceutical Research and Development. 2019;7(3):59-66.

48. Arulprakasajothi M, Elangovan K, Chandrasekhar U, Suresh S. Performance study of conical strip inserts in tube heat exchanger using water based titanium oxide nanofluid. Thermal Science. 2018;22(1 Part B):477-85.

49. Wang S-W, Lin Y-K, Fang J-Y, Lee R-S. Photo-responsive polymeric micelles and prodrugs: synthesis and characterization. RSC advances. 2018;8(51):29321-37.

50. A Rao D, Cote B, Stammet M, M Al Fatease A, WG Alani A. Evaluation of the stability of resveratrol Pluronic® micelles prepared by solvent casting and simple equilibrium methods. Pharmaceutical Nanotechnology. 2016;4(2):120-5.

51. Pervez S, Nasir F, Hidayatullah T, Khattak MA, Alasmari F, Zainab SR, et al. Transdermal Delivery of Glimepiride: A Novel Approach Using Nanomicelle-Embedded Microneedles. Pharmaceutics. 2023;15(8):2019.

52. Suvarna KS, Layton C, Bancroft JD. Bancroft's theory and practice of histological techniques: Elsevier health sciences; 2018.

53. Deyrieux AF, Wilson VG. In vitro culture conditions to study keratinocyte differentiation using the HaCaT cell line. Cytotechnology. 2007;54:77-83.



APPENDICES

Appendix 1. Copyright guideline of CC-BY license version 4.0



CC BY 4.0 DEED

Attribution 4.0 International

Canonical URL : <https://creativecommons.org/licenses/by/4.0/>

[See the legal code](#)

You are free to:

Share — copy and redistribute the material in any medium or format for any purpose, even commercially.

Adapt — remix, transform, and build upon the material for any purpose, even commercially.

The licensor cannot revoke these freedoms as long as you follow the license terms.

Under the following terms:

Attribution — You must give **appropriate credit**, provide a link to the license, and **indicate if changes were made**. You may do so in any reasonable manner, but not in any way that suggests the licensor endorses you or your use.

No additional restrictions — You may not apply legal terms or **technological measures** that legally restrict others from doing anything the license permits.

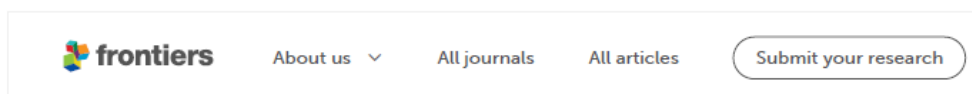
Notices:

You do not have to comply with the license for elements of the material in the public domain or where your use is permitted by an applicable **exception or limitation** .

No warranties are given. The license may not give you all of the permissions necessary for your intended use. For example, other rights such as **publicity, privacy, or moral rights** may limit how you use the material.



Appendix 2. Copyright guideline of Frontiers Journal under CC-BY 4.0 License



Policies and publication ethics

Frontiers' policies

Open access and copyright

All Frontiers articles from July 2012 onwards are published with open access under the Creative Commons [CC-BY license](#) (the current version is CC-BY, version 4.0). This means that the author(s) retains copyright, but the content is free to download, distribute, and adapt for commercial or non-commercial purposes, given appropriate attribution to the original article.

Policies and ...

Open Access a...

Authorship and...

Plagiarism and ...

Corrections an...

Conflicts of int...


Funding

Research Ethics

Data and Mater...



Appendix 3. Copyright guideline of Journal of Complementary and Traditional Medicine under CC-BY 4.0 License



ScienceDirect

Journal of Traditional and Complementary Medicine

Open access

	8.5 CiteScore	4.5 Impact Factor
--	------------------	----------------------

[Submit your article](#)

[Guide for authors](#)

Menu

Open access information

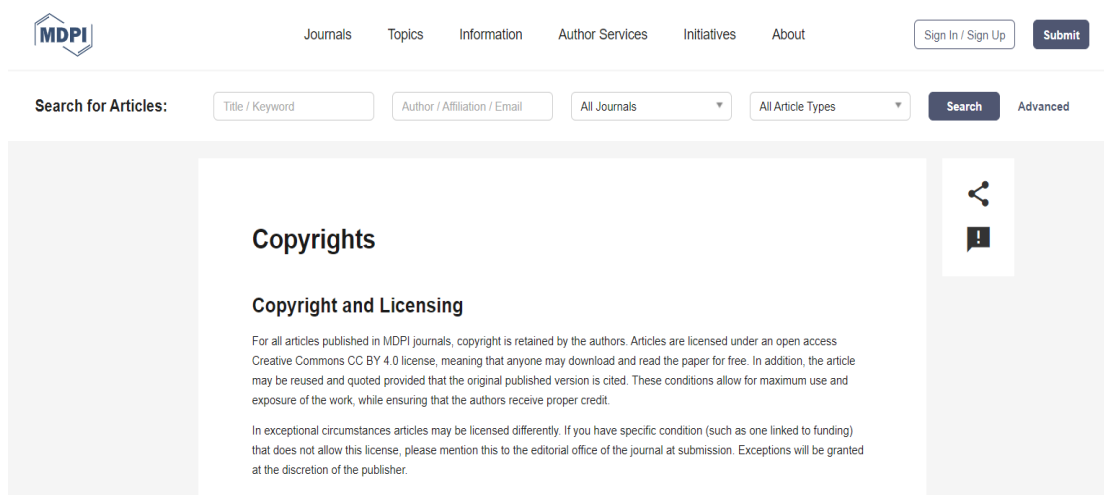
This journal is a peer reviewed, open access journal.
Peer review under the responsibility of Center for Food and Biomolecules, National Taiwan University
Open access funded by Ministry of Health and Welfare

User rights

All articles published open access will be immediately free for everyone to read, download, copy, and distribute. Permitted third party reuse is defined by your choice of one of the following user licenses/the following user license:

Creative Commons Attribution-NonCommercial-NoDerivs (CC BY-NC-ND):
Allows users to copy and distribute the Article, provided this is not done for commercial purposes and further does not permit distribution of the Article if it is changed or edited in any way, and provided the user gives appropriate credit (with a link to the formal publication through the relevant DOI), provides a link to the license, and that the licensor is not represented as endorsing the use made of the work. The full details of the license are available at <https://creativecommons.org/licenses/by-nc-nd/4.0/>.

Appendix 4. Copyright guideline of *Molecules* (MDPI) Journal under CC-BY 4.0 License



The screenshot displays the MDPI website interface. At the top left is the MDPI logo. The navigation menu includes: Journals, Topics, Information, Author Services, Initiatives, and About. On the right, there are buttons for 'Sign In / Sign Up' and 'Submit'. Below the navigation is a search bar with the text 'Search for Articles:' and four input fields: 'Title / Keyword', 'Author / Affiliation / Email', 'All Journals' (dropdown), and 'All Article Types' (dropdown). To the right of the search bar are 'Search' and 'Advanced' buttons.

Copyrights

Copyright and Licensing

For all articles published in MDPI journals, copyright is retained by the authors. Articles are licensed under an open access Creative Commons CC BY 4.0 license, meaning that anyone may download and read the paper for free. In addition, the article may be reused and quoted provided that the original published version is cited. These conditions allow for maximum use and exposure of the work, while ensuring that the authors receive proper credit.

In exceptional circumstances articles may be licensed differently. If you have specific condition (such as one linked to funding) that does not allow this license, please mention this to the editorial office of the journal at submission. Exceptions will be granted at the discretion of the publisher.

On the right side of the page, there are social sharing icons for a share symbol and a speech bubble with an exclamation mark.



VITA

NAME

Miss Su Sundee Myint

**INSTITUTIONS
ATTENDED**

University of South Australia

PUBLICATION

Myint, S.S.; Laomeephol, C.; Thamnium, S.; Chamni, S.; Luckanagul, J.A. Hyaluronic Acid Nanogels: A Promising Platform for Therapeutic and Theranostic Applications. *Pharmaceutics* 2023, 15, 2671.

<https://doi.org/10.3390/pharmaceutics15122671>

AWARD RECEIVED

University Merit Award 2018

University Merit Award 2017



จุฬาลงกรณ์มหาวิทยาลัย
CHULALONGKORN UNIVERSITY